DOI: 10.1002/ejic.200700721

Asymmetric Induction and Configurational Stability at the Metal Centre in Half-Sandwich (η^6-*p*-Cymene)ruthenium(II) and (η^5-C_5Me_5)rhodium(III) Complexes Containing Chiral N-N* Ligands with Different Rigidity and Flexibility

Maria Saporita,[a] Giovanni Bottari,[a] Giovanna Brancatelli,[a] Dario Drommi,[a] Giuseppe Bruno,[a] and Felice Faraone*[a]

Keywords: Half-sandwich complexes / Bidentate N ligands / Diastereoselectivity / Ruthenium / Rhodium

The half-sandwich chelate complexes [Ru(η^6-*p*-cymene)(N-N*)Cl]X (X = Cl, PF_6) and [Rh(η^5-C_5Me_5)(N-N*)Cl]X (X = SbF_6, PF_6; N-N* = (S_a)-**1** and (S_a)-**2**] have been prepared by treating the complexes [{Ru(η^6-*p*-cymene)Cl_2}$_2$] and [{Rh(η^5-C_5Me_5)Cl_2}$_2$] with the bidentate N-N* chiral ligands in their enantiomerically pure form. The ligands contain rigid 2-pyridinyl or 8-quinolinyl skeletons and the C_2-symmetric chiral framework *trans*-2,5-dimethylpyrrolidinyl or (+)-(*S*)-2,2′-(2-azapropane-1,3-diyl)-1,1′-binaphthalene. The chelate complexes [Ru(η^6-*p*-cymene)(N-N*)Cl]Cl and [Rh(η^5-C_5Me_5)(N-N*)Cl]SbF_6 [N-N* = (S_a)-**1** and (S_a)-**2**] were obtained in CH_3OH or $CHCl_3$, with 100% diastereomeric excess, in the absolute configurations (S_a,S_{Ru}) and (S_a,R_{Rh}), respectively; the ligands (*R*,*R*)-**3** and (*R*,*R*)-**4** gave the corresponding products as pairs of diastereomers with high *de*. A kinetic effect is present during the formation of the ruthenium and rhodium chelate complexes. The (S_a,R_{Rh}) absolute configuration of [Rh(η^5-C_5Me_5)(N-N*)Cl]PF_6 [N-N* = (S_a)-**1** and (S_a)-**2**], which were obtained as a single diastereomer, was assigned by X-ray diffraction determination of their molecular structures. The nucleophilic substitution reaction of chloride by iodide in [Ru(η^6-*p*-cymene)(N-N*)Cl]PF_6 [N-N* = (S_a)-**1** and (S_a)-**2**], in methanol at 328 K, occurs with retention of configuration at the metal centre, and a possible mechanism is proposed on the basis of kinetic measurements. The results indicate a striking analogy between the isoelectronic complexes [Ru(η^6-*p*-cymene)(N-N*)Cl]PF_6 and [Rh(η^5-C_5Me_5)(N-N*)Cl]SbF_6 containing the same N-N* chiral ligand. A rationalisation of the results is proposed on the basis of X-ray diffraction analysis and density functional calculations.
(© Wiley-VCH Verlag GmbH & Co. KGaA, 69451 Weinheim, Germany, 2008)

Introduction

Optically active organometallic complexes have attracted much interest because they are powerful tools for the development of new asymmetric catalytic reactions.[1] Half-sandwich complexes with a three-legged piano stool structure which contain ligands that are different from each other generate metal-centred chirality, and the presence of a coordinated enantiomerically pure chiral ligand induces the formation of a pair of diastereomers which differ in their optical configuration at the metal centre.[1d,2] Although a significant number of complexes with these properties have been synthesised, their application as catalysts is very limited since racemisation at the stereogenic metal centre often takes place during the reaction, and control of the stereochemistry by the metal centre does not occur. Control of the conformational stability at the metal centre is therefore an important area of research.[3]

We have reported[4,5] previously on the synthesis of [Ru(η^6-*p*-cymene)(η^1-P-N*)Cl_2] [where P-N* is a chiral (β-aminoalkyl)phosphane, (β-aminoalkyl)phosphonito, (8-quinolinyl)phosphonito or (8-quinolinyl)phosphito ligand] and [Rh(η^5-C_5Me_5)(P-N*)Cl_2] [where P-N* is a chiral (8-quinolinyl)phosphonito or (8-quinolinyl)phosphito ligand] complexes and on the chelation process of the *P*-coordinated enantiomerically pure chiral ligand P-N*, which affords the corresponding chelate complexes [Ru(η^6-*p*-cymene)(P-N*)Cl]Cl and [Rh(η^5-C_5Me_5)(P-N*)Cl]Cl with high stereoselectivity. For example, the reaction of the P-N* ligand (*R*)-8-(3,5-dioxa-4-phosphacyclohepta[2,1-*a*:3,4-*a*′]dinaphthalen-4-yl)quinoline [(*R*)-**2**] with [{Ru(η^6-*p*-cymene)Cl_2}$_2$] and [{Rh(η^5-C_5Me_5)Cl_2}$_2$] affords the chelate complexes [Ru(η^6-*p*-cymene)(*R*-**2**)Cl]Cl and [Rh(η^5-C_5Me_5)(*R*-**2**)Cl]Cl, with the latter being obtained with 100% diastereoisomeric excess.

Herein we report the synthesis of the isoelectronic half-sandwich organometallic complexes [Ru(η^6-*p*-cymene)(N-N*)Cl]X (X = Cl, PF_6) and [Rh(η^5-C_5Me_5)(N-N*)Cl]X (X = SbF_6, PF_6; N-N* = (S_a)-**1** and (S_a)-**2**] and the thermodynamic and kinetic control of the stereoselectivity of their formation. The pairs of chiral N-N* bidentate ligands (Fig-

[a] Dipartimento di Chimica Inorganica, Chimica Analitica e Chimica Fisica dell'Università di Messina,
Salita Sperone 31, Vill. S. Agata, 98166 Messina, Italy
Fax: +39-90-393-756
E-mail: ffaraone@unime.it

 © 2008 Wiley-VCH Verlag GmbH & Co. KGaA, Weinheim

ure 1) have different rigidity and flexibility, and we focus on the efficiency of these N-N* chiral ligands in the induction of diastereoselectivity and configurational stability at the stereogenic metal centre of isoelectronic half-sandwich ruthenium(II) and rhodium(III) chiral complexes.

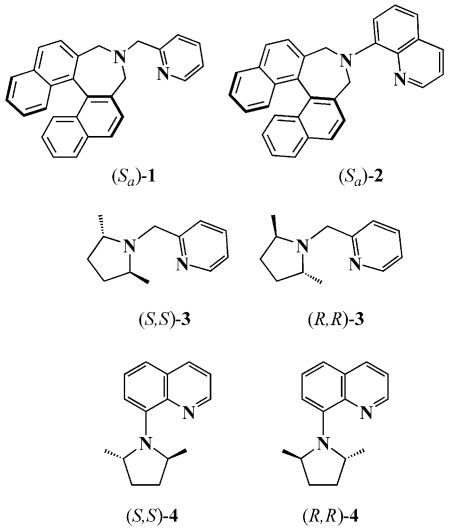

Figure 1. Ligands used in this paper.

Results

Ligands

The N-N*chiral ligands used in this study are shown in Figure 1. Some of them have been used in the synthesis of organometallic palladium complexes that catalyse asymmetric allylic alkylation[6] and stereocontrolled CO/alkene copolymerisation reactions.[7] They contain a rigid 2-pyridinyl or 8-quinolinyl skeleton and the C_2-symmetric chiral framework *trans*-2,5-dimethylpyrrolidinyl or (+)-(*S*)-2,2′-(2-azapropane-1,3-diyl)-1,1′-binaphthalene. The ligand arms, which have electronically different N-donor atoms, are separated by one sp^2- or sp^3-carbon atom spacer; this gives different rigidity and flexibility in similar ligands.

The ligands (*R*,*R*)-**3** and (*R*,*R*)-**4** are reported here for the first time and have been synthesised according to the procedure used to obtain the related enantiomers (*S*,*S*)-**3** and (*S*,*S*)-**4**, by treating the cyclic (2*S*,5*S*)-2,5-hexanediol sulfate with 2-(aminomethyl)pyridine or 8-aminoquinoline, respectively, in a molar ratio of 1:1.8 in thf solution under reflux. (*R*,*R*)-**3** is a yellow oil, while (*R*,*R*)-**4** is a yellow crystalline solid. Ligands (*R*,*R*)-**3** and (*R*,*R*)-**4** have been characterised by elemental analysis and ^{1}H NMR spectroscopy (see Experimental Section).

Synthesis of [Ru(η^6-*p*-cymene)(N-N*)Cl]X Complexes [X = Cl, PF_6; N-N* = (S_a)-1, (S_a)-2, (*R*,*R*)-3, (*R*,*R*)-4]

The [Ru(η^6-*p*-cymene)(N-N*)Cl]Cl complexes were obtained by adding the enantiomerically pure N-N* ligand, in methanol solution, to a solution of [{Ru(η^6-*p*-cymene)-Cl_2}$_2$] in the same solvent, using a complex/ligand molar ratio of 1:2. The colour of the solution turned from red to dark green upon addition of the ligand. After about 1 h, the starting ruthenium(II) complex was completely converted into the products [Ru(η^6-*p*-cymene)(N-N*)Cl]Cl as a pair of diastereoisomers that differ in the configuration at the stereogenic metal centre; workup afforded the [Ru(η^6-*p*-cymene)(N-N*)Cl]Cl complexes **5**–**8** [N-N* = (S_a)-**1**, (S_a)-**2**, (*R*,*R*)-**3**, (*R*,*R*)-**4**, respectively] as dark yellow solids. Addition of H_4NPF_6 to the complexes in a 1:1 molar ratio, in dichloromethane solution, gave complexes [Ru(η^6-*p*-cymene)(N-N*)Cl]PF_6 (**5a**–**8a**). All complexes **5**–**8** and **5a**–**8a** were characterised by elemental analysis, conductivity measurements and ^{1}H NMR spectroscopy (see Experimental Section). Table 1 reports the diastereomeric ratio of complexes **5**–**8**, in methanol, at the end of the reaction, as estimated by integration of the peaks observed in the ^{1}H NMR spectra (CD_3OD) at 298 K due to the *p*-cymene methyl group. For example, the spectrum of complex **5** shows two peaks at δ = 2.03 and 1.96 ppm, respectively, which integrate in a 75:25 ratio, whereas complex **7** shows peaks at δ = 2.10 and 1.94 ppm, respectively, in a ratio of 88:12.

Table 1. Diastereomeric ratio for ruthenium and rhodium half-sandwich complexes determined by integration of the peaks relative to the ^{1}H NMR arene signals.

Complex		(S_a)-**1**	(S_a)-**2**	(*R*,*R*)-**3**	(*R*,*R*)-**4**
[(η^6-*p*-cymene)Ru(N-N*)Cl]Cl	[a]	75:25	100	88:12	75:25
	[b]	100	100	94:6	75:25
[(η^5-C_5Me_5)Rh(N-N*)Cl]SbF_6	[a]	100	100	85:15	91:9
	[b]	100	100	85:15	91:9
[(η^5-C_5Me_5)Rh(N-N*)Cl]PF_6	[c]	100	80:20	–	–
	[d]	100	100	–	–

[a] Values at the end of the reaction in CD_3OD. [b] Values several days after the end of the reaction in CD_3OD. [c] Values at the end of the reaction in $CDCl_3$. [d] Values several days after the end of the reaction in $CDCl_3$.

The observed diastereomeric ratio can be correlated to a kinetic effect. In fact, on standing, the diastereomeric ratio of the solution containing the pair of diastereoisomers of products **5**–**8** changes until, after several days in some cases, it reaches 100% of the final value (*de* = 100%; Table 1). This was found to occur when allowing the pair of diastereoisomers of complexes **5** and **6**, which contain ligands (S_a)-**1** and (S_a)-**2**, respectively, to stand in $CHCl_3$ or CH_3OH solution. This did not occur, however, for complexes **7** and **8**, which contain ligands (*R*,*R*)-**3** and (*R*,*R*)-**4**, respectively – the diastereomeric ratio of their CH_3OH solutions did not change significantly with time. The low stability of $CHCl_3$ or CH_3OH solutions of **7** and **8** over a prolonged time prevented their pairs of diastereoisomers from being separated.

A crystallographic determination of the absolute configuration of the diastereoisomers of [Ru(η^6-*p*-cymene)-(N-N*)Cl]X [X = Cl, PF_6; N-N* = (S_a)-**1** and (S_a)-**2**] complexes was not possible because no suitable crystals were obtained. However, a multinuclear one- and two-dimen-

 © 2008 Wiley-VCH Verlag GmbH & Co. KGaA, Weinheim

sional NMR study (^{1}H, ^{13}C, ^{13}C-^{1}H HMQC, ^{1}H-COSY and 2D-NOESY) proved to be a very useful diagnostic tool for assigning the absolute configuration at the metal centre of [Ru(η^6-*p*-cymene)(S_a-**1**)Cl]Cl (**5**), which was obtained as a single diastereomer (*de* = 100%).[8]

The 2D ^{1}H-NOESY experiment (253 K, $CDCl_3$) showed net cross peaks due to a spatial interaction between the *p*-cymene ligand coordinated to the ruthenium(II) centre and the chiral ligand (S_a)-**1**. These NOE contacts between selected protons, especially those between the signals of the α-hydrogen atom of the pyridinyl group (δ = 9.58 ppm) and the *p*-cymene methyl protons (δ = 2.03 ppm), and between the signals due to the CH_2 group of the binaphthylazepine moiety (δ = 4.46 ppm) and one of the two methyl groups of the isopropyl group (δ = 0.93 ppm), were used to determine the chiral configuration of the metal complex.

Figure 2 shows two portions of the 2D ^{1}H-NOESY spectrum where the connections between the aromatic and alkyl regions can clearly be seen, particularly the NOE cross-peak due to the contact between the α-hydrogen atom of the pyridine ring and the methyl group bonded to the arene in the *p*-cymene ligand. The spectrum also exhibits a weak contact between the proton of the sp^3-carbon spacer (δ = 4.95 ppm) and the *p*-cymene methyl group (δ = 2.03 ppm). These signals allowed us to correlate the position of the coordinated *p*-cymene ligand with respect to the binaphthylazepine and the CH_2 spacer moiety. The 2D NMR spectroscopic data of complex **5** suggest the structural configuration shown in Figure 3. The absolute configuration (*S*) at the ruthenium atom was assigned by assuming the following priority numbers: 1 (*p*-cymene), 2 (Cl), 3 (N-pyridinyl), 4 (N-azepine), which means that the diastereomer **5** has an (S_a,S_{Ru}) absolute configuration.

The determination of the absolute configuration of complex **5** by NMR spectroscopy allowed us to assign the configuration of **6**, which was again obtained as a single diastereoisomer. The similarity of the CD spectra of the dia-

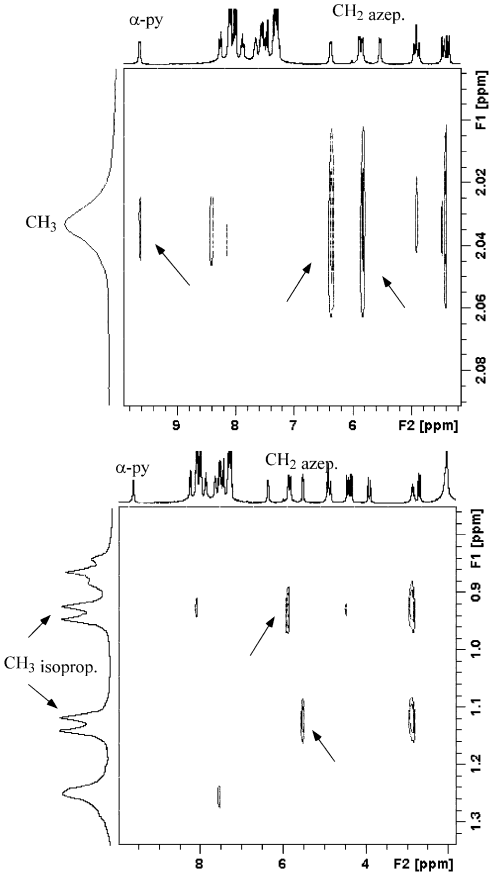

Figure 2. Two sections of the 2D ^{1}H-NOESY NMR spectrum of [Ru(η^6-*p*-cymene)(S_a-**1**)Cl]Cl. The arrows indicate the NOE contacts between the methyl groups of the *p*-cymene and α-pyridine and methylene hydrogen atoms of the ligand.

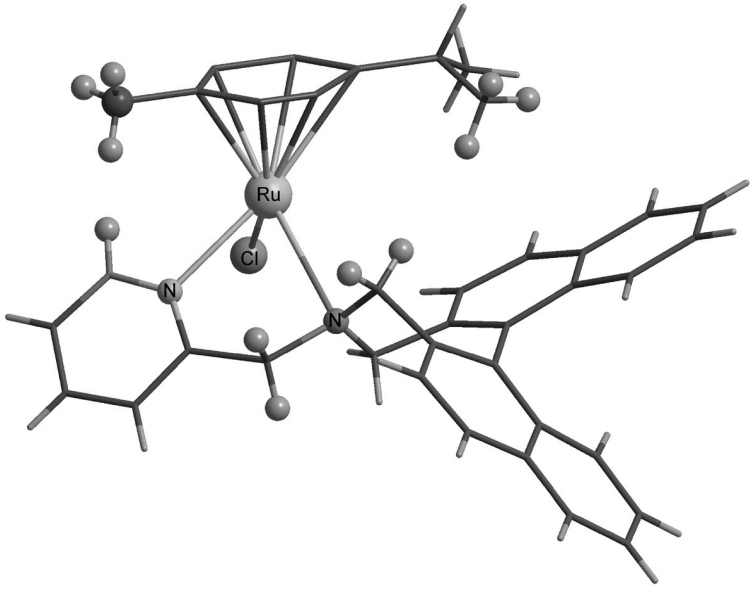

Figure 3. 3D view of [Ru(η^6-*p*-cymene)(S_a-**1**)Cl]Cl.

 © 2008 Wiley-VCH Verlag GmbH & Co. KGaA, Weinheim

stereomers of **5** and **6** (CH_3OH solution; Figure 4), which were obtained with 100% *de*, supports the conclusion that their absolute configuration in solution is the same (S_a,S_{Ru}).

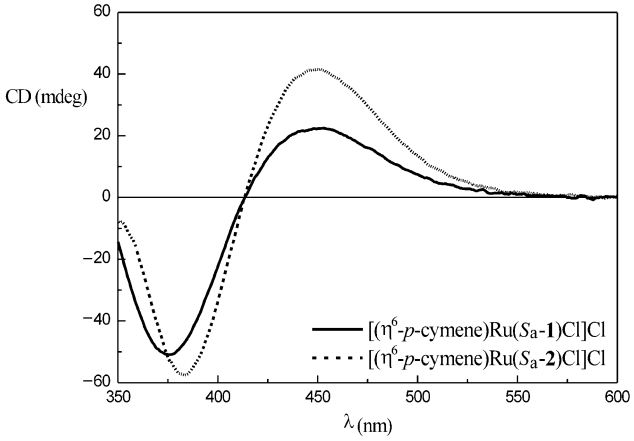

Figure 4. CD spectrum of complexes [Ru(η^6-*p*-cymene)(S_a-**1**)Cl]Cl and [Ru(η^6-*p*-cymene)(S_a-**2**)Cl]Cl. $c = 5\times10^{-4}$ M, 20 °C, CH_2Cl_2. $\Delta\varepsilon$ in L mol^{-1} cm^{-1}.

Brunner and co-workers[9] have pointed out that a comparison of CD spectra is not always an accurate method for establishing the absolute configuration of a chiral compound. However, we consider the comparison of the CD spectra of complexes containing an (S_a)-**1** or (S_a)-**2** ligand a valid method for establishing their absolute configuration due to the presence of very similar chiral chromophores.

Synthesis of [Rh(η^5-C_5Me_5)(N-N*)Cl]SbF_6 Complexes [N-N* = (S_a)-1, (S_a)-2, (*R*,*R*)-3, (*R*,*R*)-4]

Similarly to [{Ru(η^6-*p*-cymene)Cl_2}$_2$], the reaction of [{Rh(η^5-C_5Me_5)Cl_2}$_2$] with chiral N-N* ligands affords the complexes [Rh(η^5-C_5Me_5)(N-N*)Cl]Cl, which were isolated as their SbF_6^- salts after further treatment with $NaSbF_6$. The reactions were performed by adding the ligand N-N* and $NaSbF_6$, in methanol, to a solution of [{Rh(η^5-C_5Me_5)Cl_2}$_2$] in the same solvent with a complex/ligand/Sb molar ratio of 1:2:2. The reaction mixture was refluxed for 2 h and then left at room temperature. After this time, [{Rh(η^5-C_5Me_5)Cl_2}$_2$] had been completely converted into the reaction product. Workup afforded the products [Rh(η^5-C_5Me_5)(N-N*)Cl]SbF_6 [**9**–**12**; N-N* = (S_a)-**1**, (S_a)-**2**, (*R*,*R*)-**3** and (*R*,*R*)-**4**, respectively] as yellow solids that are air-stable in the solid state for a long time. Complexes **9**–**12** were characterised by elemental analysis, conductivity measurements and ^{1}H NMR spectroscopy. Complexes **9** and **10**, which contain ligands (S_a)-**1** and (S_a)-**2**, respectively, were obtained with 100% *de*, as shown by the presence of peaks for the C_5Me_5 moiety in the ^{1}H NMR spectra in CD_3OD. Figures 5 and 6 show a comparison of the CD spectra of Ru and Rh half-sandwich complexes bearing the same N-N* chiral ligand and different absolute configurations at the metal centre.

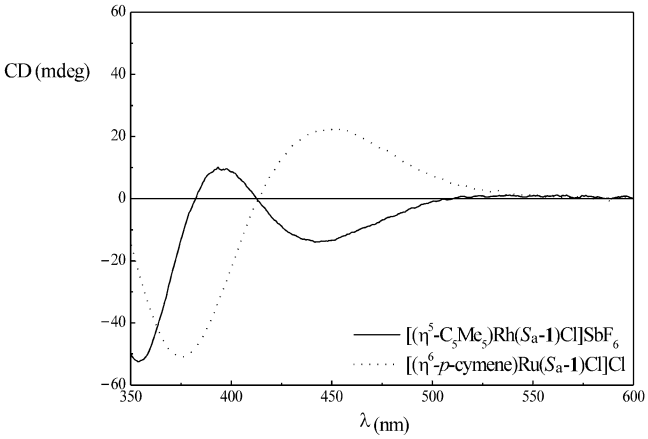

Figure 5. CD spectrum of complexes [Ru(η^6-*p*-cymene)(S_a-**1**)Cl]Cl and [Rh(η^5-C_5Me_5)(S_a-**1**)Cl]SbF_6. $c = 5\times10^{-4}$ M, 20 °C, CH_2Cl_2. $\Delta\varepsilon$ in L mol^{-1} cm^{-1}.

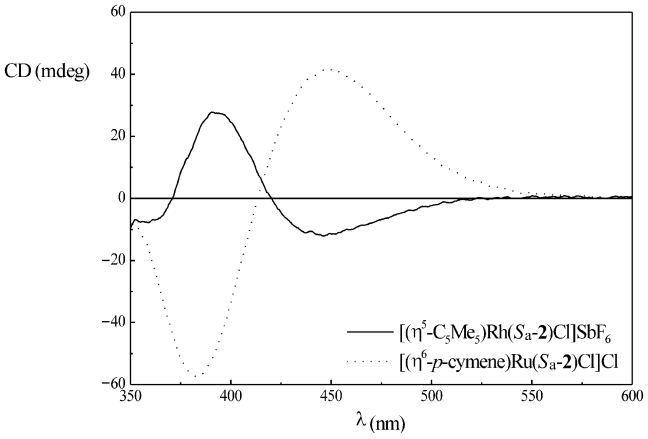

Figure 6. CD spectrum of complexes [Ru(η^6-*p*-cymene)(S_a-**2**)Cl]Cl and [Rh(η^5-C_5Me_5)(S_a-**2**)Cl]SbF_6. $c = 5\times10^{-4}$ M, 20 °C, CH_2Cl_2. $\Delta\varepsilon$ in L mol^{-1} cm^{-1}.

In contrast to **9** and **10**, complexes [Rh(η^5-C_5Me_5)(*R*,*R*-**3**)Cl]SbF_6 (**11**) and [Rh(η^5-C_5Me_5)(*R*,*R*-**4**)Cl]SbF_6 (**12**) were obtained with diastereomeric ratios of 85:15 and 91:9, respectively (Table 1). These ratios remain nearly unchanged on allowing complexes **11** and **12** to stand in CH_3OH or $CHCl_3$ for about 20 h due to their limited stability in solution with respect to the other complexes **9** and **10**. The different temperature conditions used did not allow us to compare the kinetic and thermodynamic effects on the diastereomeric excess induced by the same ligand in the reactions of [{Ru(η^6-*p*-cymene)Cl_2}$_2$] and [{Rh(η^5-C_5Me_5)Cl_2}$_2$] with the chiral N-N* ligands. In fact, because of the high temperature required in the reactions with [{Rh(η^5-C_5Me_5)Cl_2}$_2$] a very fast configurational inversion at the metal centre in the minor isomer, formed initially due to a kinetic effect, could occur. Fortunately, modifying the synthetic procedure by operating at room temperature in CH_3CN allowed us to obtain complexes **9** and **10** as their PF_6^- salts **9a** and **10a**. However, although **9a** was obtained with a diastereomeric excess of 100%, **10a** gave a pair of diastereomers in an 80:20 ratio, as shown by the ^{1}H NMR

 © 2008 Wiley-VCH Verlag GmbH & Co. KGaA, Weinheim

spectra in $CDCl_3$. After several days, a $CHCl_3$ solution of this complex afforded **10a** as a single diastereomer (Table 1). We were not able to obtain the corresponding PF_6 salts of **11** and **12** by the same procedure. Crystals of complexes **9** and **10a** were obtained by slow concentration of a $CHCl_3$ solution of the complex. An X-ray crystallographic study proved that the absolute configuration of these diastereoisomers is (S_a,R_{Rh}).

Crystal and Molecular Structures of [Rh(η^5-C_5Me_5)(S_a-1)-Cl]SbF_6 (9) and [Rh(η^5-C_5Me_5)(S_a-2)Cl]PF_6 (10a)

Views of the molecular structures of **9** and **10a**, together with the atom numbering schemes, are shown in Figures 7 and 8, respectively; selected bond lengths and angles are reported in Table 2.

Molecule **9** crystallises in the non-centrosymmetric space group $P2_1$. The asymmetric unit contains a cationic rhodium moiety and a disordered SbF_6^- anion. The coordination environment at the metal centre displays a three-legged piano stool involving the η^5-C_5Me_5 ligand [the mean planes of C_5Me_5 and N(1)–Cl(1)–N(2) are roughly parallel at 173.3(3)°], two nitrogen atoms of the (S_a)-**1** chelating ligand and a chlorine atom. If the centroid of the η^5-C_5Me_5 ligand is considered as a single site [Rh–C bond lengths range from 2.12(1) to 2.20(1) Å; Rh(1)–centroid 1.78(4) Å], the coordination geometry can also be described as chiral pseudo-tetrahedral. The absolute configuration at the rhodium atom was assigned by assuming the following priority numbers: 1 (C_5Me_5), 2 (Cl), 3 (N-pyridinyl), 4 (N-azepine). Thus, the absolute configuration at the rhodium metal centre is (*R*) and that of the diastereomer **9** is (S_a,R_{Rh}).

The Rh(1)–N(1)–C(5)–C(6)–N(2) chelate ring is not perfectly planar as C(6) deviates from the plane by –0.422(9) Å. This five-membered ring has an envelope conformation, as seen from an analysis of the puckering coordinates[10] [E_5 with ϕ_2 = –42(1)° and q_2 = 0.482(8)], and a bite angle of 77.1(3)°. The Rh(1)–Cl(1), Rh(1)–N(1) and Rh(1)–N(2) bond lengths are 2.411(2), 2.106(8) and 2.250(7) Å, respectively. The difference in length between the Rh–N bonds is mainly due to the different hybridisation of the two N atoms [sp^2 vs. sp^3 for N(1) and N(2), respectively].[11,12] Some methyl carbon atoms of the C_5Me_5 moiety deviate from the mean plane constituted by the five carbon atoms in the ring: [C(34) –0.15(1), C(35) –0.22(1), C(36) –0.07(1), C(37) –0.14(1), C(38) –0.13(1) Å]. The C(35)

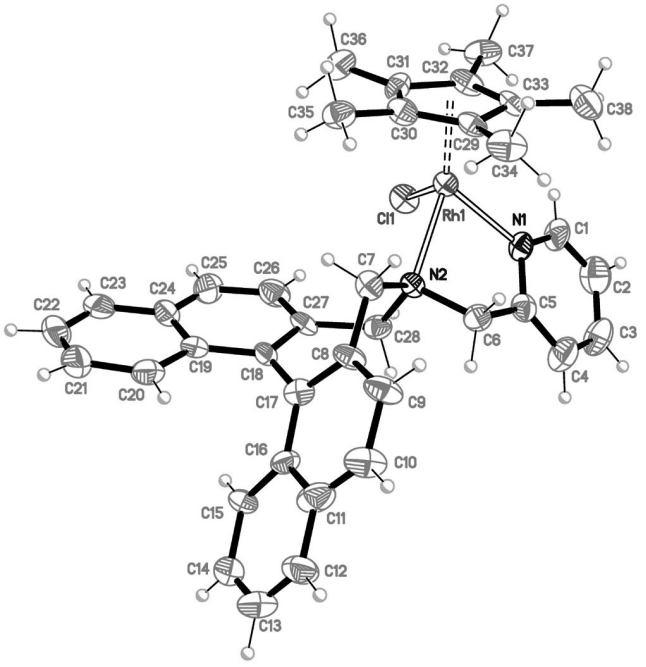

Figure 7. ORTEP view of the crystal structure of **9** with atom numbering scheme and ellipsoids at the 30% probability level. The SbF_6 anion has been omitted for clarity.

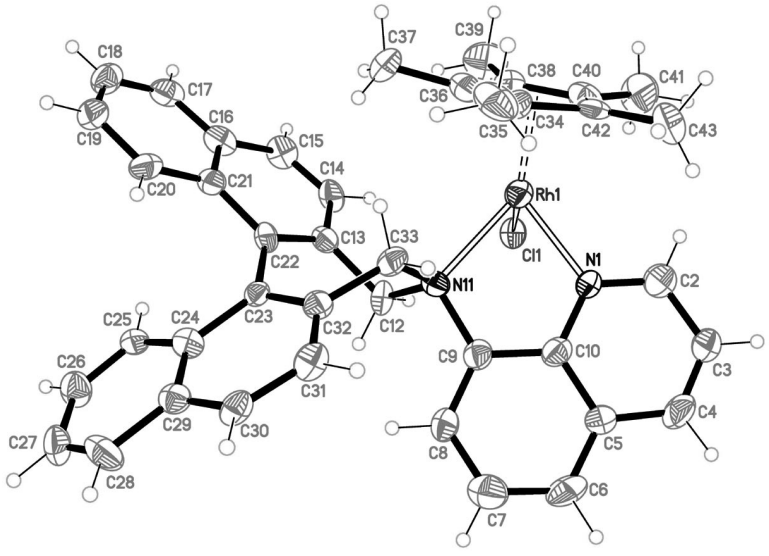

Figure 8. ORTEP view of the crystal structure of **10a** with atom numbering scheme and ellipsoids at the 30% probability level. The SbF_6 anion has been omitted for clarity.

 © 2008 Wiley-VCH Verlag GmbH & Co. KGaA, Weinheim

Table 2. Selected bond lengths [Å] and angles [°] for **9** and **10a**.

9			
Rh(1)–N(1)	2.106(8)	Rh(1)–C(29)	2.146(8)
Rh(1)–N(2)	2.250(7)	Rh(1)–C(30)	2.20(1)
Rh(1)–Cl(1)	2.411(2)	Rh(1)–C(31)	2.17(1)
N(1)–C(1)	1.32(1)	Rh(1)–C(32)	2.12(1)
N(2)–C(7)	1.49(1)	Rh(1)–C(33)	2.137(9)
N(2)–C(28)	1.536(1)	N(2)–C(6)	1.46(1)
N(1)–Rh(1)–Cl(1)	84.5(2)	N(2)–Rh(1)–Cl(1)	95.9(2)
N(1)–Rh(1)–N(2)	77.1(3)	C(1)–N(1)–C(5)	116.8(9)
C(6)–N(2)–C(7)	109.5(7)	N(2)–C(6)–C(5)	112.0(8)
10a			
Rh(1)–N(1)	2.070(6)	Rh(1)–C(34)	2.197(8)
Rh(1)–N(11)	2.275(7)	Rh(1)–C(36)	2.191(9)
Rh(1)–Cl(1)	2.427(2)	Rh(1)–C(38)	2.167(9)
N(1)–C(2)	1.31(1)	Rh(1)–C(40)	2.17(1)
N(11)–C(9)	1.48(1)	Rh(1)–C(42)	2.199(9)
N(11)–C(12)	1.53(1)	N(11)–C(33)	1.508(9)
N(1)–Rh(1)–Cl(1)	84.2(2)	N(11)–Rh(1)–Cl(1)	90.2(2)
N(1)–Rh(1)–N(11)	79.0(3)	C(2)–N(1)–C(10)	120.2(7)
C(9)–N(11)–C(33)	110.8(6)	C(10)–C(9)–N(11)	118.2(8)

atom is more shifted owing to an intramolecular contact with C(7) of the azepine moiety [3.33(1) Å]. The N(1)–Rh(1)–Cl(1) and N(2)–Rh(1)–Cl(1) angles are 84.5(2)° and 95.9(2)°, respectively, and show a greater steric effect of the chiral azepine moiety with respect to the pyridinyl framework.

Complex **10a** crystallises in the chiral space group $P2_12_12_1$. The asymmetric unit contains one cationic rhodium moiety and one disordered PF_6 anion in a 1:1 ratio, with one chloroform solvate molecule. As for **9**, the metal centre displays a three-legged piano-stool structure involving an η^5-C_5Me_5 ligand [the five Rh–C bond lengths are within the range 2.167(9)–2.199(9) Å; Rh(1)–centroid 1.75(3) Å], a Cl atom and two N atoms of the (S_a)-**2** chelating ligand. The coordination geometry can also be described as chiral pseudo-tetrahedral.

The priority numbers are the same as for **9**, which means that the absolute configuration at the rhodium metal centre is (*R*) and that of the diastereomer **10a** is (S_a,R_{Rh}). The five-membered Rh(1)–N(1)–C(10)–C(9)–N(11) ring is perfectly planar and shows an N(1)–Rh(1)–N(11) bite angle of 79.0(3)°, which is slightly larger than that found in **9**. The N(1)–Rh(1)–Cl(1) angles [84.2(2)°] is smaller than the N(11)–Rh(1)–Cl(1) angle [90.2(2)°] due to the greater steric effect of the azepine moiety with respect to the 8-quinolinyl moiety. The Rh(1)–Cl(1), Rh(1)–N(1) and Rh(1)–N(11) bond lengths are 2.427(2), 2.070(6) and 2.275(7) Å, respectively. The Rh(1)–N(11) distance is slightly longer than that found in **9**, probably because of a more significant steric hindrance exerted by the binaphthyl group.

The two naphthyl moieties are planar and form a dihedral angle of 57.6(1)°. Because of the presence of this bulky group, some of the methyl C atoms deviate strongly from the mean plane of the η^5-C_5Me_5 ligand [C(35) –0.21(1), C(37) –0.21(1), C(39) –0.20(1), C(41) –0.08(1), C(43) –0.07(1) Å]. The C(35) and C(37) atoms are shifted out of the plane due to close contacts with the binaphthyl group [3.36(1)–3.58(1) Å]. Similar deviations have been found for structures containing an (η^5-C_5Me_5)Rh moiety with bulky ligands in the first coordination sphere of the rhodium atom in the CSD.[11] The orientation of the azepine chiral framework in **9** and **10a** is significantly different. Thus, the binaphthyl moiety of the (S_a)-**1** ligand in complex **9** points downwards, towards the less congested side of the molecule, to minimise the steric interactions with C_5Me_5. This is possible owing to the flexibility of the ligand due to the presence of the sp^3 spacer C(6). In **10a**, however, the quinolinyl sp^2 spacer C(9) gives rigidity to the ligand and positions the binaphthyl moiety of (S_a)-**2** ligand upwards. The orientation of the binaphthyl group in **9** also exerts a minor steric interaction on the coordination plane formed by the Cl and the N atoms with respect to the orientation assumed in **10a**. This is supported by the difference between the N(1)–Rh(1)–Cl(1) and N(2)–Rh(1)–Cl(1) angles of 11.4° in **9** and the N(1)–Rh(1)–Cl(1) and N(11)–Rh(1)–Cl(1) angles of 6.0° in **10a**.

Nucleophilic Substitution between [Ru(η^6-*p*-cymene)(N-N*)-Cl]PF_6 [N-N* = (S_a)-1 and (S_a)-2] and *n*Bu_4NI

We confirmed that complexes (S_a,S_{Ru})-**5a** and (S_a,S_{Ru})-**6a** undergo nucleophilic substitution of the coordinated chloride by iodide with retention of configuration at the metal centre:

(S_a,S_{Ru})-[Ru(η^6-*p*-cymene)(N-N*)Cl]PF_6 + R_4NI → (S_a,R_{Ru})-[Ru(η^6-*p*-cymene)(N-N*)I]PF_6 + R_4NCl

N-N* = (S_a)-**1** and (S_a)-**2**; R = *n*-butyl

The nucleophilic substitution reaction of chloride by iodide was carried out in methanol, at 328 K, using an excess of *n*Bu_4NI. The course of the nucleophilic substitution reaction was monitored by recording the ^{1}H NMR spectra of samples of the solution with time. This allowed us to establish that a single diastereomer of the corresponding [Ru(η^6-*p*-cymene)(N-N*)I]$^+$ cation was formed. The assignment of the configuration at the ruthenium atom in the chloride and iodide derivatives came from a comparison of their CD spectra (Figure 9), which show very similar curves.

The presence of iodide at the site previously occupied by the chloride does not change the mutual disposition of the atoms coordinated to the ruthenium atom but modifies the priority sequence: 1 (I), 2 (*p*-cymene), 3 (N-quinolinyl), 4 (N-azepine). Thus, we conclude that substitution reactions of [Ru(η^6-*p*-cymene)(N-N*)Cl]PF_6 [N-N* = (S_a)-**1** and (S_a)-**2**] by *n*Bu_4NI occur with retention of the configuration although the absolute configuration at the ruthenium atom in the reaction product is (*R*). No epimerisation or racemisation at the ruthenium centre was observed on allowing a methanol solution of [Ru(η^6-*p*-cymene)(N-N*)I]PF_6 to stand for several days.

Replacement of the coordinated chloride in **5a** and **6a** by iodide can take place through a dissociative or associative mechanism. An associative mechanism is considered unlikely for nucleophilic substitution reactions that occur with

 © 2008 Wiley-VCH Verlag GmbH & Co. KGaA, Weinheim

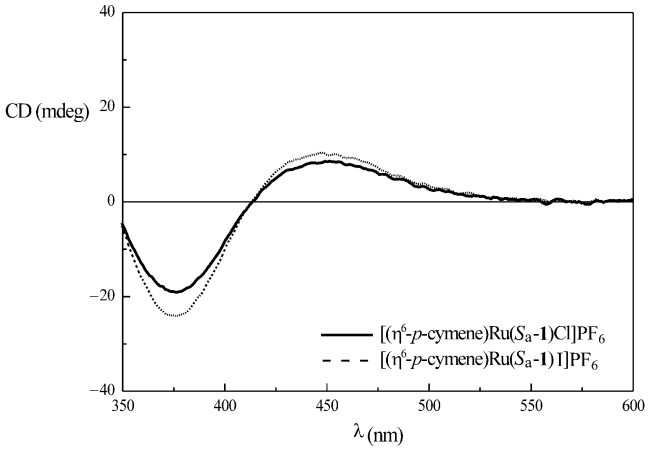

Figure 9. CD spectrum of complexes [Ru(η^6-*p*-cymene)(S_a-**1**)Cl]-PF_6 and [Ru(η^6-*p*-cymene)(S_a-**1**)I]PF_6. $c = 5\times10^{-4}$ M, 20 °C, CH_2Cl_2. $\Delta\varepsilon$ in L mol^{-1} cm^{-1}.

retention of configuration at the metal centre because it implies formation either of a 20-electron or an (η^4-C_5Me_5)Ru^{II} species. However, such a mechanism has been supported by experimental data[13] and theoretical studies.[14] A dissociative mechanism has been proposed for either substitution reactions affording epimerisation and/or racemisation of the products or in those that occur with retention of the configuration at the metal centre.[15] Generally, the results are best explained by mechanisms involving initial dissociation of a coordinated ligand, with possible anchimeric assistance,[15,16] as a rate-determining step, to give chiral pyramidal intermediates which can interconvert through a planar species. The conformational stability of such species has been established by theoretical studies,[17] and experimental results[16,18] have shown that the stereochemical outcome can also be determined after the dissociative rate-determining step and that it can be influenced by the steric features of the incoming ligand. In fact, experimental data show that, in some cases, increasing the bulk of the incoming ligand also increases the diastereomeric excess; this supports an associative I*a*-type interchange mechanism.[18]

We have found previously[4] that the kinetics, under pseudo-first-order conditions, of the chelation process in the neutral species [Ru(η^6-arene)(η^1-P-N*)Cl_2] [P-N* = (β-aminoalkyl)phosphanes; arene = benzene, hexamethylbenzene, *p*-cymene], in $CDCl_3$ solution containing variable amounts of methanol, or of alcohols with different hydrogen-bonding properties, follows a first-order course, and the k_{obs} values are linearly correlated to the nucleophile (methanol) concentration, with no significant intercept. These kinetic results led us to propose a mechanism in which the rate-determining step of the process is solvolysis of the starting complex in methanol. Subsequent fast closure of the chelate ring by coordination of the nitrogen atom to the ruthenium(II) centre determines the stereoselectivity of the process.[4]

Since a similar mechanism, in which the chloride dissociation step is assisted by the methanol solvent, could be active in the reactions studied here, we carried out a kinetic measurement of the nucleophilic substitution reactions of Cl^- by I^- at 328 K, under pseudo-first-order conditions with respect to I^-, in $CHCl_3$ solution containing variable amounts of methanol. We found that the kinetics, in a large range of methanol concentrations, follow a first-order course and that the k_{obs} values are linearly correlated to the methanol concentration ([MeOH] = 12.25 M, $k_{obs} = 2\times10^{-5}$ s^{-1}; [MeOH] = 19.6 M, $k_{obs} = 5\times10^{-5}$ s^{-1}; [MeOH] = 24.5 M, $k_{obs} = 7\times10^{-5}$ s^{-1}; Figure 10). This linear correlation loses validity at low methanol concentrations, and the intercept becomes > 0, thereby indicating competition between $CHCl_3$ and CH_3OH; the kinetic law becomes more complicated in these low methanol concentration ranges.

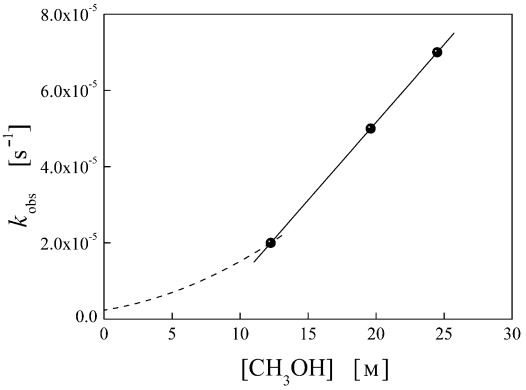

Figure 10. Plots of k_{obs} vs. [CH_3OH] for the nucleophilic substitution reactions of coordinated chloride in the complexes [Ru(η^6-*p*-cymene)(N-N*)Cl]PF_6. T = 328 K.

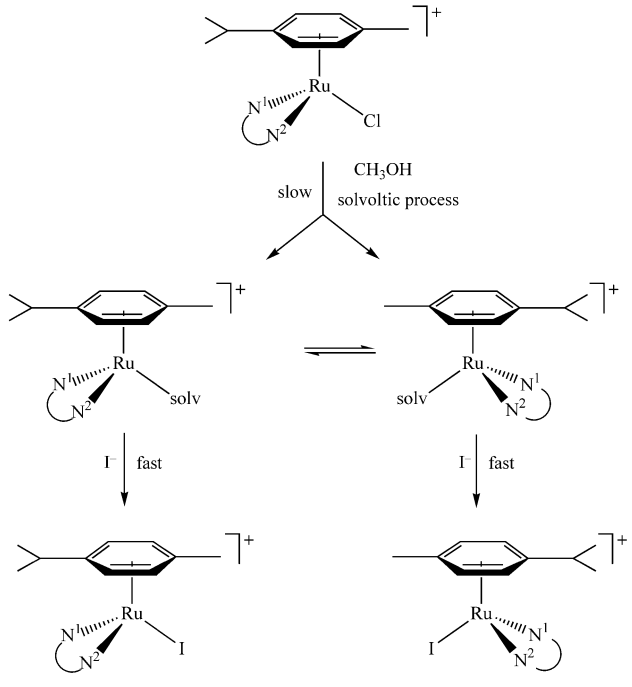

Scheme 1.

 © 2008 Wiley-VCH Verlag GmbH & Co. KGaA, Weinheim

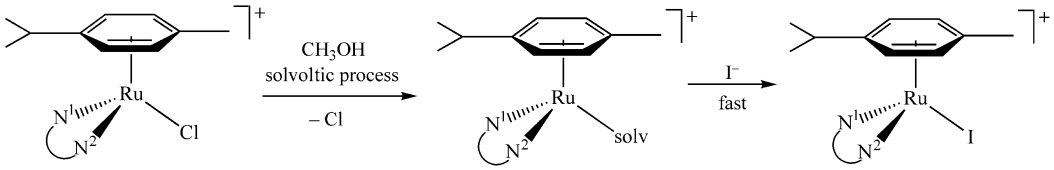

Scheme 2.

In methanol solution, these experimental data support a mechanism in which the chloride dissociation process, which leads to a cationic (*p*-cymene)ruthenium(II) solvento species, occurs by a hydrogen-bond interaction between the coordinated chloride ion and methanol. As the ruthenium(II) atom is a stereogenic centre, this solvento species can be present, in principle, as a pair of diastereomers [(S_a,S_{Ru}) and (S_a,R_{Ru})], which are in equilibrium. Formation of the diastereomeric solvento species (S_a,R_{Ru}) implies a configuration inversion in the 16-electron pyramidal intermediate, and the presence of the (S_a,R_{Ru}) solvento species leads to a competitive reaction pathway to the formation of the reaction product with retention of configuration. The reactivity of the diastereomeric solvento species intermediates, which is influenced by the N-N* ligand, therefore determines the diastereomeric ratio. This proposed mechanism (Scheme 1) recalls that proposed by other authors who do not take the role of the solvent into consideration.[16]

It has been reported previously that [Ru(η^6-*p*-cymene)(N-N*)Cl]PF_6 [N-N* = (S_a)-**1**, (S_a)-**2**] complexes are formed as a single diastereomer [(S_a,S_{Ru})-**5** and (S_a,S_{Ru})-**6**, respectively] due to their very much higher thermodynamic configurational stability with respect to the corresponding (S_a,R_{Ru}) diastereomers. It is very likely that such a situation is also the case for the solvento species [Ru(η^6-*p*-cymene)(N-N*)(CH_3OH)]$^{2+}$ [N-N* = (S_a)-**1**, (S_a)-**2**], which will also be present as a single (S_a,S_{Ru}) diastereomer and will give the corresponding iodide [Ru(η^6-*p*-cymene)-(N-N*)I]PF_6, in a fast step, with retention of configuration (Scheme 2). As demonstrated below for the complexes reported in this work, the diastereoselectivity appears mainly to be determined by the chiral chelating ligand.

Further kinetic studies are in progress in order to gain a greater understanding of the intimate stereochemical mechanism of these reactions.

Theoretical Calculations

Density functional calculations were performed on models of the pairs of diastereoisomers (RR_a,R_{Ru})-/(RR_a,S_{Ru})-[Ru(*p*-cymene)(*R*,*R*-**4**)Cl]$^+$ and (S_a,R_{Rh})-/(S_a,S_{Rh})-[Rh(η^5-C_5Me_5)(S_a-**2**)Cl]$^+$. These models reproduce the features of the complete structures of the diastereoisomers, namely the coordination environment of the ruthenium or rhodium atom, the chelate ring and the core of the complex, in a reliable way. The adopted atom numbering is reported in Figure 11; selected computed bond lengths, angles and relative energies for the pairs of diastereoisomers are listed in Table 3.

The focus here is on a study of the model structures to check their reliability in reproducing the geometry at the central metal atom in the complexes and to characterise the existing conformational changes due to steric interactions. The complexity and number of atoms in the considered structures prevents the use of ab initio methods for all the diastereomers of interest, therefore we performed density calculations on molecules containing the (S_a)-**2** ligand but with a biphenyl moiety instead of a binaphthyl one. We have verified in a previous work[4] that the difference between real binaphthyl species and the biphenyl-optimised model in density functional calculations is not significant. The optimised structure of the cationic diastereomer (S_a,R_{Rh})-[Rh(η^5-C_5Me_5)(S_a-**2**)Cl]$^+$ was found to be in good agreement with the crystal structure of (S_a,R_{Rh})-[Rh(η^5-C_5Me_5)(S_a-**2**)Cl]PF_6 (**10a**), thereby indicating the validity of the performed simplification on the chiral backbone (Figure 12). Relevant distances and angles in the computed structure of (S_a,R_{Rh})-[Rh(η^5-C_5Me_5)(S_a-**2**)Cl]$^+$ are given in Table 3 and are clearly in accordance with those found for **10a**.

The energy difference between the pair of diastereomers for [Rh(η^5-C_5Me_5)(S_a-**2**)Cl]$^+$, which differ in the absolute

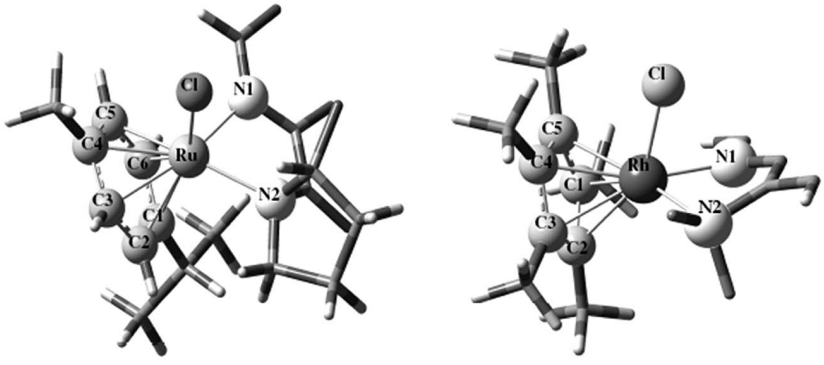

Figure 11. Atom numbering scheme of [Ru(*p*-cymene)(*R*,*R*-**4**)Cl]$^+$ and [Rh(η^5-C_5Me_5)(S_a-**2**)Cl]$^+$ core models.

 © 2008 Wiley-VCH Verlag GmbH & Co. KGaA, Weinheim

Table 3. Relative energies [kJ mol^{-1}] and selected structural parameters for (S_a,R_{Rh})-[Rh(η^5-C_5Me_5)(S_a-**2**)Cl]$^+$ (X-ray) and the models (S_a,R_{Rh})-[Rh(η^5-C_5Me_5)(S_a-**2**)Cl]$^+$, (S_a,S_{Rh})-[Rh(η^5-C_5Me_5)(S_a-**2**)Cl]$^+$, (RR_a,R_{Ru})-[Ru(*p*-cymene)(*R*,*R*-**4**)Cl]$^+$ and (RR_a,S_{Ru})-[Ru(*p*-cymene)(*R*,*R*-**4**)Cl]$^+$.

	(S_a,R_{Rh})-[Rh(η^5-C_5Me_5)(S_a-**2**)Cl]$^+$[a]	(S_a,R_{Rh})-[Rh(η^5-C_5Me_5)(S_a-**2**)Cl]$^+$	(S_a,S_{Rh})-[Rh(η^5-C_5Me_5)(S_a-**2**)Cl]$^+$	(RR_a,R_{Ru})-[Ru(*p*-cymene)(*R*,*R*-**4**)Cl]$^+$	(RR_a,S_{Ru})-[Ru(*p*-cymene)(*R*,*R*-**4**)Cl]$^+$
E(rel.)		0	31.02	0	18.11
M–N1	2.070(6)	2.0475	2.0745	2.0546	2.0509
M–N2	2.275(7)	2.2269	2.2258	2.2222	2.2528
M–Cl	2.427(2)	2.4283	2.4449	2.4152	2.4026
M–C1	2.197(8)	2.2384	2.2522	2.3379	2.3045
M–C2	2.191(9)	2.2882	2.2425	2.2889	2.2404
M–C3	2.167(9)	2.2465	2.1982	2.2927	2.2658
M–C4	2.17(1)	2.1851	2.2212	2.3227	2.2942
M–C5	2.199(9)	2.2294	2.2797	2.2022	2.2264
M–C6				2.2227	2.2181
M–centroid	1.75(3)	1.8882	1.8564	1.7441	1.7575
N1–M–N2	79.0(3)	80.12	78.38	79.80	76.38
N1–M–Cl	84.2(2)	83.33	83.54	82.37	88.78
N2–M–Cl	90.2(2)	91.46	85.26	84.09	90.25
N1–M–centroid	129(1)	131.85	135.27	132.57	127.52
N2–M–centroid	137(1)	134.28	138.03	134.54	133.79
Cl–M–centroid	121(1)	119.90	117.41	124.86	124.37

[a] X-ray determination.

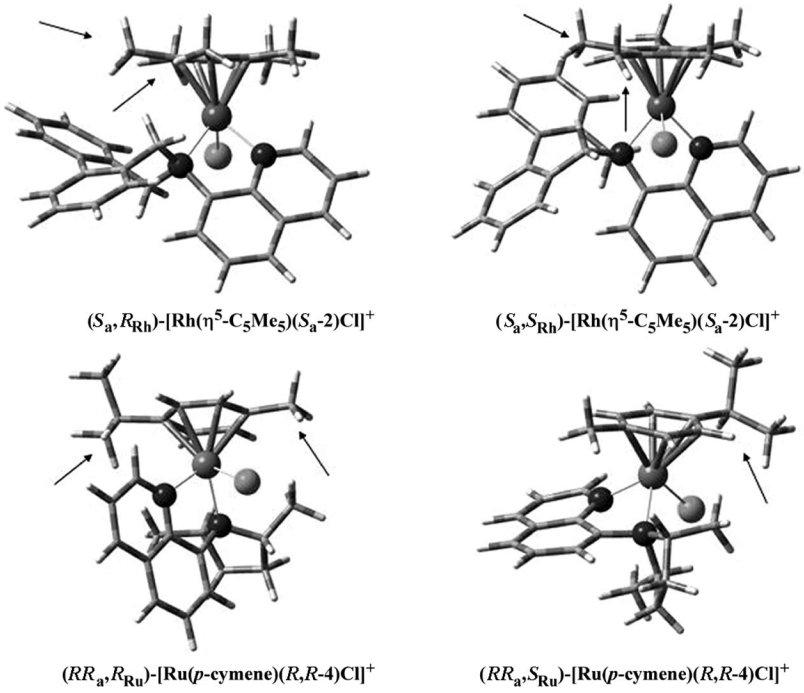

Figure 12. View of the (S_a,R_{Rh})-[Rh(η^5-C_5Me_5)(S_a-**2**)Cl]$^+$, (S_a,S_{Rh})-[Rh(η^5-C_5Me_5)(S_a-**2**)Cl]$^+$, (RR_a,R_{Ru})-[Ru(*p*-cymene)(*R*,*R*-**4**)Cl]$^+$ and (RR_a,S_{Ru})-[Ru(*p*-cymene)(*R*,*R*-**4**)Cl]$^+$ models.

configuration at the metal centre, was found to be 31.02 kJ mol^{-1}, with (S_a,R_{Rh})-[Rh(η^5-C_5Me_5)(S_a-**2**)Cl]$^+$ being the most stable; this result is in agreement with the experimental evidence that this complex is formed as a single diastereomer as its PF_6 salt.

The energy difference between the pair of diastereomers (RR_a,S_{Ru})-/(RR_a,R_{Ru})-[Ru(*p*-cymene)(*R*,*R*-**4**)Cl]$^+$, was found to be 18.11 kJ mol^{-1}, which indicates only a minor difference in the thermodynamic stability of the diastereomers and a lower capability of the (*R*,*R*-**4**) ligand to induce diastereoselectivity than (S_a)-**2**.

The calculated geometrical parameters reported in Table 3 give similar bond lengths for Rh–N^1 (2.075–2.048 Å), Rh–N^2 (2.226–2.227 Å), Ru–N^1 (2.055–2.051 Å), Ru–N^2 (2.222–2.253 Å), Rh–Cl (2.445–2.428 Å) and Ru–Cl (2.403–2–415 Å); the metal–nitrogen bond lengths are in the range normally found for Rh–N_{sp^3} and Rh–N_{sp^2} or Ru–N_{sp^3} and Ru–N_{sp^2} bonds, respectively.[12,19]

 © 2008 Wiley-VCH Verlag GmbH & Co. KGaA, Weinheim

The computed bite angle (N^1–M–N^2) is almost the same for coordinated (S_a)-**2** and (*R*,*R*)-**4**, both of which contain an 8-quinolinyl skeleton. The differences between the N^1–M–Cl and N^2–M–Cl angles are indicative of the steric hindrance of the ligand arms and can be correlated to the presence of the sp^3-azepine N^2-donor in (S_a)-**2** and the sp^3-*trans*-2,5-dimethyl-pyrrolidinyl N^2-donor in (*R*,*R*)-4; both ligands contain an 8-quinolinyl sp^2-carbon spacer. The computed N^1–Rh–Cl and N^2–Rh–Cl angles differ by 8.1° in (S_a,R_{Rh})-[Rh(η^5-C_5Me_5)(S_a-**2**)Cl]$^+$, while this value is 6.0° from the structural determination of **10a** by X-ray diffraction. This difference becomes just 1.72° in the computed (S_a,S_{Rh})-[Rh(η^5-C_5Me_5)(S_a-**2**)Cl]$^+$ diastereomer due to a structural rearrangement of the central core that leads to longer Rh–Cl and Rh–N^1 bonds (2.445 and 2.075 Å, respectively).

The difference between the N^1–Rh–Cl and N^2–Rh–Cl angles in the (RR_a,S_{Ru})-/(RR_a,R_{Ru})-[Ru(*p*-cymene)(*R*,*R*-**4**)-Cl]$^+$ models is only 1.47° and 1.72°, respectively. A similarly small difference has also been found in other X-ray structures of palladium complexes with the same ligand.[20] Thus, the computed and experimental values indicate that the sp^3-azepine chiral framework exhibits a greater steric hindrance than the sp^3-*trans*-2,5-dimethylpyrrolidinyl one in the coordination sphere formed by the Cl and N-N* atoms.

Some of the atoms that form the aromatic ring coordinated to the metal centre deviate from planarity in the calculated models due to steric interactions with the N-N* ligand. Thus, the methyl carbon atom and the isopropyl group of *p*-cymene deviate significantly from the C_6H_4 plane in the (RR_a,R_{Ru})-[Ru(*p*-cymene)(*R*,*R*-**4**)Cl]$^+$ diastereomer (Figure 12) due to close contacts with the methyl carbon atom of the dimethylpyrrolidinyl moiety (3.465 Å) and a carbon atom from the quinolinyl portion, respectively, whereas in the (RR_a,S_{Ru})-[Ru(*p*-cymene)(*R*,*R*-**4**)Cl]$^+$ diastereomer the isopropyl carbon atom of *p*-cymene is tilted most out of the plane (distance from the mean plane: 0.173Å) because of interactions with the dimethylpyrrolidinyl moiety (3.316 Å).

The distortions of the C_5Me_5 methyl carbon atoms in the (S_a,R_{Rh})-/(S_a,S_{Rh})-[Rh(η^5-C_5Me_5)(S_a-**2**)Cl]$^+$ models are similar to those found in the crystal structure of **10a** [calculated range: 0.091–0.227 Å; experimental range: 0.08(1)–0.21(1) Å].

Discussion and Conclusions

Several conclusions may be drawn from this study. The results indicate a striking analogy between isoelectronic [Ru(η^6-*p*-cymene)(N-N*)Cl]Cl and [Rh(η^5-C_5Me_5)(N-N*)-Cl]SbF_6 complexes containing the same N-N* chiral ligand. Ligands (S_a)-**1** and (S_a)-**2** give the corresponding [Ru(η^6-*p*-cymene)(N-N*)Cl]X (X = Cl, PF_6) and [Rh(η^5-C_5Me_5)(N-N*)Cl]X (X = SbF_6, PF_6) complexes with a quantitative conversion of the starting material and 100% *de*, whereas ligands (*R*,*R*)-**3** and (*R*,*R*)-**4** give the corresponding ruthenium and rhodium complexes as a pair of diastereomers with high *de*. This emphasises the ability of ligands (S_a)-**1** and (S_a)-**2** to induce high diastereoselectivity and even to give the corresponding half-sandwich products with 100% *de*. The configurational stability of the metal centre in the ruthenium complexes **5a** and **6a** has been verified in the nucleophilic substitution reaction of coordinated chloride by iodide. This finding indicates a very different thermodynamic stability for the pair of diastereomers formed with these ligands. In fact, due to a kinetic effect, complexes [Ru(η^6-*p*-cymene)(S_a-**1**)Cl]Cl (**5**) and [Ru(η^6-*p*-cymene)(S_a-**2**)Cl]Cl (**6**) are obtained with a *de* lower than 100%, although their CH_3OH or $CHCl_3$ solutions afford a single diastereomer on standing. A kinetic effect has also been shown in the reaction of [{Rh(η^5-C_5Me_5)Cl_2}$_2$] with (S_a)-**2** at room temperature with CH_3CN as solvent, whereas under the same experimental conditions complex [Rh(η^5-C_5Me_5)(S_a-**1**)Cl]PF_6 (**9a**) is obtained directly with 100% *de* (Table 1).

A comparison between the reactions of (S_a)-**1** and (S_a)-**2** with [{Ru(η^6-*p*-cymene)Cl_2}$_2$] and [{Rh(η^5-C_5Me_5)Cl_2}$_2$] indicates a greater thermodynamic stability of the rhodium complexes. Furthermore, the complexes [Ru(η^6-*p*-cymene)(N-N*)Cl]Cl (**7** and **8**) and [Rh(η^5-C_5Me_5)(N-N*)Cl]SbF_6 [**11** and **12**; N-N* = (*R*,*R*)-**3** and (*R*,*R*)-**4**, respectively] show striking analogies in that they are always obtained as a pair of diastereomers and with high diastereomeric excess (greater in the rhodium complexes), no racemisation processes occur upon standing at room temperature in $CHCl_3$ or CH_3OH solution for about 30 h. Complexes **8** and mainly **12** have limited stability in solution and lose the coordinated ligand (*R*,*R*)-**4** at room temperature after about 1 d.

These considerations strongly support the viewpoint that the different abilities of ligands (S_a)-**1** and (S_a)-**2** with respect to (*R*,*R*)-**3** and (*R*,*R*)-**4** to induce diastereoselectivity and configurational stability at the metal centre in cationic half-sandwich ruthenium(II) and rhodium(III) complexes must be related to the structural features of the coordinated ligands. The aim of the study was to gain insight into the effects of the rigidity and flexibility of the coordinated chelating ligands on the efficiency of the diastereoselective synthesis and configurational stability of half-sandwich ruthenium and rhodium complexes. The pairs of ligands (S_a)-**1**/(S_a)-**2** and (*R*,*R*)-**3**/(*R*,*R*)-**4** differ from each other only in their C_2-symmetrical chiral frameworks [(+)-(*S*)-2,2′-(2-azapropane-1,3-diyl)-1,1′-binaphthalene (azepine) for the former pair and *trans*-2,5-dimethylpyrrolidinyl for the latter]. Consequently, the difference in the diastereoselectivity observed using these pairs of ligands must be related to the presence of these chiral moieties.

The molecular structures of complexes **9** and **10a**, as determined by X-ray diffraction, indicate that the orientation of the (+)-(*S*)-2,2′-(2-azapropane-1,3-diyl)-1,1′-binaphthalene moiety in ligands (S_a)-**1** and (S_a)-**2** is affected by the rigidity and flexibility of the N-N* ligand. In complex **9**, for example, the sp^3-carbon spacer induces a flexibility in (S_a)-**1** that allows the (+)-(*S*)-2,2′-(2-azapropane-1,3-diyl)-1,1′-binaphthalene moiety to be directed towards the less congested part of the molecule, whereas in complex **10a** the

 © 2008 Wiley-VCH Verlag GmbH & Co. KGaA, Weinheim

chiral framework present in (S_a)-**2** is directed towards the upper part of the molecule due to the rigidity induced by the sp^2 quinolinyl spacer. This produces repulsive interactions in **10a** that force a tilting of the η^5-C_5Me_5 ring. A similar orientation of the chiral framework with respect to the coordination plane has been found in the complex [Pd(S_a-**2**)(CH_3)Cl].[7]

We were not able to obtain crystals of half-sandwich Ru or Rh complexes containing ligands (*R*,*R*)-**3** or (*R*,*R*)-**4** suitable for an X-ray structural determination; however, DFT calculations performed on the diastereoisomeric pair (RR_a,S_{Ru})- and (RR_a,R_{Ru})-[Ru(*p*-cymene)(*R*,*R*-**4**)Cl]$^+$ give useful information on the stereochemistry of the *trans*-2,5-dimethylpyrrolidinyl chiral framework. The computed molecular structures of these diastereoisomers (Figure 12) show that the *trans*-2,5-dimethylpyrrolidinyl chiral framework is oriented almost orthogonal to the coordination and quinolinyl planes. Determination of the molecular structures of complexes [Pd(N-N*)Cl_2] [N-N* = (*R*,*R*)-**3** and (*R*,*R*)-**4**] by X-ray diffraction confirms this orientation of the *trans*-2,5-dimethylpyrrolidinyl chiral framework for both (*R*,*R*)-**3** and (*R*,*R*)-**4**, thereby indicating that the rigidity and flexibility of the ligand in these palladium complexes do not modify the stereochemical configuration of the ligands in any significant way.[20] This orientation of the *trans*-2,5-dimethylpyrrolidinyl chiral framework is very likely present in the ruthenium and rhodium half-sandwich complexes **7/8** and **11/12**. As a result, the *trans*-2,5-dimethylpyrrolidinyl chiral moiety is oriented towards the upper part of the coordination plane, close to the η^6-*p*-cymene or η^5-C_5Me_5 ligands. Strong repulsive interactions between the *trans*-2,5-dimethylpyrrolidinyl moiety and the η^6-*p*-cymene group in the related computed ruthenium diastereomers (RR_a,R_{Ru})- and (RR_a,S_{Ru})-[Ru(*p*-cymene)(*R*,*R*-**4**)Cl]$^+$ have been found by DFT calculations. Complexes containing ligands (*R*,*R*)-**3** and (*R*,*R*)-**4** are markedly less stable in solution than the related complexes with ligands (S_a)-**1** and (S_a)-**2**, and they lose their chelating coordinated ligand within a few hours.

Thus, although the different rigidity and flexibility of ligands (S_a)-**1** and (S_a)-**2** determine the orientation of the binaphthylazepine moiety, the results reported in this work cannot be explained in terms of these ligand features, which are the same for both pairs of ligands, but by the stereochemical arrangement of the coordinated ligand in the half-sandwich metal complex. This determines the different thermodynamic stabilities of the pair of diastereomers and the activation energy of the process that induces the diastereoselectivity, as confirmed by the calculated energy values.

This work has also reported an unusual reaction that takes place with retention of configuration at the metal centre: diastereomers (S_a,S_{Ru})-**5a** and (S_a,S_{Ru})-**6a** undergo nucleophilic substitution of the coordinated chloride by iodide with retention of the configuration at the ruthenium centre. We have proposed a possible chloride dissociation reaction mechanism for these reactions assisted by the methanol solvent (see above).

Experimental Section

General Methods: All manipulations were carried out under argon using standard Schlenk techniques. Freshly distilled solvents were used throughout and dried by standard procedures. Published methods were used to prepare the complexes (+)-(S_a)-2,2′-[2-(2-methylpyridyl)-2-azapropane-1,3-diyl]-1,1′-binaphthalene[21] [(S_a)-**1**] and (–)-(S_a)-2,2′-[(7-quinolinyl)-2-azapropane-1,3-diyl]-1,1′-binaphthalene [(S_a)-**2**].[6] (+)-(*R*,*R*)-2-[(2,5-Dimethylpyrrodin-1-yl)-methyl]pyridine [(*R*,*R*)-**3**] and (+)-(*R*,*R*)-8-(2,5-dimethylpyrrodin-1-yl)quinoline [(*R*,*R*)-**4**] were prepared from (2*S*,5*S*)-2,5-hexanediol sulfate as reported in the literature.[6] All other reagents were purchased from Sigma–Aldrich or Strem and were used as supplied. Silica gel 60 (220 ± 440 mesh) and neutral aluminium oxide activity grade 1 (70–290 mesh) purchased from Fluka were used for column chromatography. Optical rotations were recorded with a JASCO P-1010 Automatic Polarimeter in a 1-dm cell (*c* in g/100 mL), and CD spectra were recorded with a Jasco J-810 spectropolarimeter. Conductivity measurements were performed with a Metrohm 644 conductimeter. 1D and 2D NMR experiments were carried out with a Bruker AMX R300 spectrometer. ^{1}H NMR spectra were referenced to internal tetramethylsilane. Standard pulse sequences were employed for phase-sensitive (TPPI method) ^{1}H-2D NOESY and ^{13}C-^{1}H correlation (HMQC) studies.[22] Elemental analyses were performed by Redox s.n.c., Cologno Monzese, Milano. All calculations were carried out using the Gaussian G03W program package.[23] The structures and bonding parameters were computed at the density functional (DFT) B3LYP level of theory, using Becke's exchange functional, which includes the Slater exchange along with corrections involving the density gradient[24] and Perdew and Wang's gradient-corrected correlation functional.[24,25]

Synthesis of the Half-Sandwich Complexes [(η^6-*p*-cymene)Ru(N-N*)Cl]Cl [5–8; N-N* = (S_a)-1, (S_a)-2, (*R*,*R*)-3 and (*R*,*R*)-4, respectively]: These complexes were synthesised as follows. The ligand (0.196 mmol) was added to a solution of [{$RuCl_2$(*p*-cymene)}$_2$] (60 mg, 0.098 mmol) in MeOH (10 mL), and the colour of the solution changed from red to dark green. After about 1 h, the solvent was evaporated under vacuum and the residue filtered through a pad of Celite. The filtrate was then concentrated and the solid residue precipitated from CH_2Cl_2/hexane to give the complex as a brownish product that was washed with hexane (3 × 10 mL) and dried under an inert gas.

[(η^6-*p*-cymene)Ru(S_a-1)Cl]Cl (5): Yield: 70% (95.5 mg, 0.138 mmol). ^{1}H NMR ($CDCl_3$): major isomer: δ = 9.58 (d, ^3J = 5 Hz, 1 H, H α-pyridine), 6.43 (d, ^3J = 6 Hz, 1 H, Ar-H, *p*-cymene), 5.86 (d, ^3J = 6 Hz, 1 H, Ar-H, *p*-cymene), 5.80 (d, ^3J = 6 Hz, 1 H, Ar-H, *p*-cymene), 5.55 (d, ^3J = 6 Hz, 1 H, Ar-H, *p*-cymene), 5.00 (d, ^2J = 12 Hz, 1 H, CH_2 ligand), 4.95 (d, ^2J = 15 Hz, 1 H, CH_2 ligand), 4.46 (d, ^2J = 15 Hz, 1 H, CH_2 ligand), 4.35 (d, ^2J = 12 Hz, 1 H, CH_2 ligand), 3.93 (d, ^2J = 15 Hz, 1 H, CH_2 ligand), 2.71 (d, ^2J = 12 Hz, 1 H, CH_2 ligand), 2.88 (m, 1 H, CH *isopropyl*, *p*-cymene), 2.03 (s, 3 H, CH_3, *p*-cymene), 1.15 (d, ^3J = 7 Hz, 3 H, CH_3 *isopropyl*, *p*-cymene), 0.93 (d, ^3J = 7 Hz, 3 H, CH_3 *isopropyl*, *p*-cymene); minor isomer: δ = 9.05 (d, ^3J = 5 Hz, 1 H, H α-pyridine), 5.51 (d, ^2J = 14 Hz, 1 H, CH_2 ligand), 5.46 (d, ^2J = 16 Hz, 1 H, CH_2 ligand), 4.18 (d, ^2J = 16 Hz, 1 H, CH_2 ligand), 3.84 (d, ^2J = 14 Hz, 1 H, CH_2 ligand), 3.59 (d, ^2J = 14 Hz, 1 H, CH_2 ligand), 2.64 (d, ^2J = 14 Hz, 1 H, CH_2 ligand), 3.00 (m, 1 H, CH *isopropyl*, *p*-cymene), 2.09 (s, 3 H, CH_3, *p*-cymene), 1.29 (d, ^3J = 7 Hz, 3 H, CH_3 *isopropyl*, *p*-cymene), 1.11 (d, ^3J = 7 Hz, 3 H, CH_3 *isopropyl*, *p*-cymene) ppm. $C_{38}H_{36}Cl_2N_2Ru$ (692.68): calcd. C 65.89, H 5.24, N 4.04; found C 68.85, H 5.56, N 4.21. Conductivity (5×10^{-4} M, CH_3OH): Λ = 68 Ω^{-1} cm^2 mol^{-1}.

 © 2008 Wiley-VCH Verlag GmbH & Co. KGaA, Weinheim

[(η⁶-*p*-cymene)Ru(*S*ₐ-2)Cl]Cl (6): Yield: 74% (53 mg, 0.072 mmol). ^{1}H NMR ($CDCl_3$): δ = 9.78 (d, ^3J = 5 Hz, 1 H, H α-quinoline), 6.86 (d, ^3J = 8 Hz, 1 H, Ar-H, *p*-cymene), 6.77 (d, ^3J = 8 Hz, 1 H, Ar-H, *p*-cymene), 5.91 (t, ^3J = 6 Hz, 2 H, Ar-H, *p*-cymene), 5.35 (d, ^2J = 12 Hz, 1 H, CH_2 ligand), 5.16 (d, ^2J = 13 Hz, 1 H, CH_2 ligand), 4.25 (d, ^2J = 13 Hz, 1 H, CH_2 ligand), 4.23 (d, ^2J = 12 Hz, 1 H, CH_2 ligand), 2.87 (m, 1 H, CH *isopropyl*, *p*-cymene), 2.11 (s, 3 H, CH_3, *p*-cymene), 1.33 (d, ^3J = 7 Hz, 3 H, CH_3 *isopropyl*, *p*-cymene), 1.18 (d, ^3J = 7 Hz, 3 H, CH_3 *isopropyl*, *p*-cymene). $C_{41}H_{36}Cl_2N_2Ru$ (728.71): calcd. C 67.58, H 4.98, N 3.84; found C 66.03, H 5.28, N 3.71. Conductivity (5×10^{-4} M, CH_3OH): Λ = 63 Ω^{-1} cm^2 mol^{-1}.

[(η⁶-*p*-cymene)Ru(*R*,*R*-3)Cl]Cl (7): Yield: 72% (34.7 mg, 0.070 mmol). ^{1}H NMR ($CDCl_3$): major isomer: δ = 9.62 (d, ^3J = 5 Hz, 1 H, H α-pyridine), 6.28 (d, ^3J = 6 Hz, 1 H, Ar-H, *p*-cymene), 5.89 (d, ^3J = 6 Hz, 1 H, Ar-H, *p*-cymene), 5.84 (d, ^3J = 6 Hz, 1 H, Ar-H, *p*-cymene), 5.73 (d, ^3J = 6 Hz, 1 H, Ar-H, *p*-cymene), 4.30 (m, 1 H, CH), 3.76 (s, 2 H, CH_2 ligand), 3.65 (m, 1 H, CH), 2.96 (m, 1 H, CH *isopropyl*, *p*-cymene), 2.47 (m, 2 H, CH_2), 2.39 (m, 2 H, CH_2), 2.15 (s, 3 H, CH_3, *p*-cymene), 1.63 (d, ^3J = 7 Hz, 3 H, CH_3 ligand), 1.33 (d, ^3J = 7 Hz, 3 H, CH_3 *isopropyl*, *p*-cymene), 1.23 (d, ^3J = 7 Hz, 3 H, CH_3 *isopropyl*, *p*-cymene), 1.03 (d, ^3J = 7 Hz, 3 H, CH_3 ligand); minor isomer: δ = 8.90 (d, ^3J = 5 Hz, 1 H, H α-pyridine), 6.36 (d, ^3J = 6 Hz, 1 H, Ar-H, *p*-cymene), 5.93 (d, ^3J = 6 Hz, 1 H, Ar-H, *p*-cymene), 5.61 (d, ^3J = 6 Hz, 1 H, Ar-H, *p*-cymene), 5.59 (d, ^3J = 6 Hz, 1 H, Ar-H, *p*-cymene), 2.77 (m, 1 H, CH *isopropyl*, *p*-cymene), 2.23 (s, 3 H, CH_3, *p*-cymene), 1.42 (d, ^3J = 7 Hz, 3 H, CH_3 ligand), 1.28 (d, ^3J = 7 Hz, 3 H, CH_3 *isopropyl*, *p*-cymene), 1.18 (d, ^3J = 7 Hz, 3 H, CH_3 *isopropyl*, *p*-cymene), 1.09 (d, ^3J = 7 Hz, 3 H, CH_3 ligand) ppm. $C_{22}H_{32}Cl_2N_2Ru$ (496.48): calcd. C 53.22, H 6.50, N 5.64; found C 51.16, H 6.37, N 5.81. Conductivity (5×10^{-4} M, CH_3OH): Λ = 81 Ω^{-1} cm^2 mol^{-1}.

[(η⁶-*p*-cymene)Ru(*R*,*R*-4)Cl]Cl (8): Yield: 70% (48 mg, 0.090 mmol). ^{1}H NMR ($CDCl_3$): δ = 10.1 (d, ^3J = 4 Hz, 1 H, H α-quinoline), 6.75 (d, ^3J = 5 Hz, 1 H, Ar-H, *p*-cymene), 5.87 (d, ^3J = 5 Hz, 1 H, Ar-H, *p*-cymene), 5.82 (d, ^3J = 6 Hz, 1 H, Ar-H, *p*-cymene), 5.74 (d, ^3J = 6 Hz, 1 H, Ar-H, *p*-cymene), 5.48 (m, 1 H, CH ligand), 4.53 (m, 1 H, CH ligand), 4.11 (m, 1 H, CH_2 ligand), 3.20 (m, 1 H, CH_2 ligand), 3.02 (m, 1 H, CH *isopropyl*, *p*-cymene), 2.91 (m, 1 H, CH_2 ligand), 2.59 (m, 1 H, CH_2 ligand), 2.28 (s, 3 H, CH_3 *p*-cymene), 2.06 (d, ^3J = 7 Hz, 3 H, CH_3 ligand), 1.34 (d, ^3J = 7 Hz, 3 H, CH_3 *isopropyl*, *p*-cymene), 1.30 (d, ^3J = 7 Hz, 3 H, CH_3 *isopropyl*, *p*-cymene), 0.63 (d, ^3J = 7 Hz, 3 H, CH_3 ligand) ppm. $C_{25}H_{32}Cl_2N_2Ru$ (532.51): calcd. C 56.39, H 6.06, N 5.26; found C 55.01, H 6.11, N 5.69. Conductivity (5×10^{-4} M, CH_3OH): Λ = 75 Ω^{-1} cm^2 mol^{-1}.

Synthesis of the Half-Sandwich Complexes [(η⁶-*p*-cymene)Ru(N-N*)Cl]PF₆ [5a–8a; N-N* = (*S*ₐ)-1, (*S*ₐ)-2, (*R*,*R*)-3 and (*R*,*R*)-4, respectively]: These complexes were synthesised as follows. A thf solution of NH_4PF_6 (0.2 mmol) was added to a solution of [(η⁶-*p*-cymene)Ru(N-N*)Cl]Cl (0.1 mmol) in thf (10 mL). After about 1 h, the solvent was evaporated under vacuum and the residue filtered through a pad of Celite. The filtrate was concentrated and the solid residue precipitated from CH_2Cl_2/hexane to give the complex as a yellow product that was washed with hexane (3 × 10 mL) and dried under an inert gas.

Synthesis of Half-Sandwich Complexes [Rh(η⁵-C₅Me₅)(N-N*)Cl]SbF₆ [9–12; N-N* = (*S*ₐ)-1, (*S*ₐ)-2, (*R*,*R*)-3 and (*R*,*R*)-4, respectively]: These complexes were synthesised as follows. A solution of the ligand (0.17 mmol) and $NaSbF_6$ (43.5 mg, 0.17 mmol) in MeOH (8 mL) was added to a solution of [{$RhCl_2Cp^*$}$_2$] (50 mg, 0.08 mmol) in MeOH (10 mL), and the mixture was heated to 70 °C for 3 h. The resulting yellow-orange solution was left to cool and was then concentrated under vacuum. The residue was dissolved in CH_2Cl_2 and filtered through a pad of Celite. Precipitation from CH_2Cl_2/hexane gave [Rh(η^5-C_5Me_5)(N-N*)Cl]SbF_6 as a yellow solid.

[Rh(η⁵-C₅Me₅)(*S*ₐ-1)Cl][SbF₆] (9): Yield: 75% (113 mg, 0.126 mmol). ^{1}H NMR ($CDCl_3$): δ = 8.63 (d, ^3J = 5 Hz, 1 H, H α-pyridine), 4.66 (d, ^3J = 12 Hz, 1 H, CH_2 ligand), 4.51 (d, ^3J = 15 Hz, 1 H, CH_2 ligand), 4.39 (s, 2 H, CH_2 ligand), 3.86 (d, ^3J = 15 Hz, 1 H, CH_2 ligand), 2.84 (d, ^3J = 12 Hz, 1 H, CH_2 ligand), 1.88 (s, 15 H, C_5Me_5) ppm. $C_{38}H_{37}ClF_6N_2RhSb$ (895.82): calcd. C 50.95, H 4.16, N 3.13; found C 49.16, H 4.12, N 3.05. Conductivity (5×10^{-4} M, CH_3OH): Λ = 84 Ω^{-1} cm^2 mol^{-1}.

[Rh(η⁵-C₅Me₅)(*S*ₐ-2)Cl]SbF₆ (10): Yield: 81% (127 mg, 0.136 mmol). ^{1}H NMR ($CDCl_3$): δ = 8.95 (d, ^3J = 5 Hz, 1 H, H α-quinoline), 5.35 (d, ^3J = 12 Hz, 1 H, CH_2 ligand), 5.04 (d, ^3J = 13 Hz, 1 H, CH_2 ligand), 4.86 (d, ^3J = 13 Hz, 1 H, CH_2 ligand), 4. 02 (d, ^3J = 12 Hz, 1 H, CH_2 ligand), 1.33 (s, 15 H, C_5Me_5) ppm. $C_{41}H_{37}ClF_6N_2RhSb$ (931.86): calcd. C 52.84, H 4.00, N 3.01; found C 52.14, H 4.00, N 3.01. Conductivity (5×10^{-4} M, CH_3OH): Λ = 81 Ω^{-1} cm^2 mol^{-1}.

[Rh(η⁵-C₅Me₅)(*R*,*R*-3)Cl]SbF₆ (11): Yield: 78% (95 mg, 0.136 mmol). ^{1}H NMR ($CDCl_3$): δ = 8.61 (d, ^3J = 6 Hz, 1 H, H α-pyridine), 1.62 (s, 15 H, C_5Me_5) ppm. $C_{22}H_{33}ClF_6N_2RhSb$ (699,62): calcd. C 37.77, H 4.75, N 4.00; found C 37.28, H 4.73, N 4.00. Conductivity (5×10^{-4} M, CH_3OH): Λ = 75 (Ω^{-1} cm^2 mol^{-1}).

[Rh(η⁵-C₅Me₅)(*R*,*R*-4)Cl]SbF₆ (12): Yield: 76% (94 mg, 0.128 mmol). ^{1}H NMR ($CDCl_3$): δ = 9.07 (d, ^3J = 4 Hz, 1 H, H α-quinoline), 1.67 (s, 15 H, C_5Me_5) ppm. $C_{25}H_{33}ClF_6N_2RhSb$ (735.65): calcd. C 40.82, H 4.52, N 3.81; found C 37.80, H 4.45, N 3.72. Conductivity (5×10^{-4} M, CH_3OH): Λ = 90 Ω^{-1} cm^2 mol^{-1}.

[Rh(η⁵-C₅Me₅)(N-N*)Cl]PF₆ Half-Sandwich Complexes 9a and 10a [N-N* = (*S*ₐ)-1 and (*S*ₐ)-2 respectively]: $AgPF_6$ (48.6 mg, 0.192 mmol) was added to a solution of [{$RhCl_2Cp^*$}$_2$] (60 mg, 0.096 mmol) in anhydrous acetonitrile (10 mL). The resulting turbid solution was filtered through Celite, and a solution of the ligand (0.192 mmol) in 5 mL of acetonitrile was added to the filtrate. The colour changed from orange to red, then became green before turning orange again. The mixture was stirred overnight, then the solvent was evaporated and the residue dissolved in CH_2Cl_2. Precipitation from CH_2Cl_2/hexane gave the complex as a light-yellow solid.

[Rh(η⁵-C₅Me₅)(*S*ₐ-1)Cl]PF₆ (9a): Yield: 71% (109 mg, 0.136 mmol). ^{1}H NMR ($CDCl_3$): δ = 8.63 (d, ^3J = 5 Hz, 1 H, H α-pyridine), 4.66 (d, ^3J = 12 Hz, 1 H, CH_2 ligand), 4.45 (d, ^3J = 15 Hz, 1 H, CH_2 ligand), 4.38 (s, 2 H, CH_2 ligand), 3.87 (d, ^3J = 15 Hz, 1 H, CH_2 ligand), 2.85 (d, ^3J = 12 Hz, 1 H, CH_2 ligand), 1.49 (s, 15 H, C_5Me_5) ppm. $C_{38}H_{37}ClF_6N_2PRh$ (805.04): calcd. C 56.69, H 4.63, N 3.48; found C 53.82, H 4.62, N 3.38. Conductivity (5×10^{-4} M, CH_3OH): Λ = 84 Ω^{-1} cm^2 mol^{-1}.

[Rh(η⁵-C₅Me₅)(*S*ₐ-2)Cl]PF₆ (10a): Yield: 68% (109 mg, 0.130 mmol). ^{1}H NMR ($CDCl_3$): major isomer: δ = 8.98 (d, ^3J = 5 Hz, 1 H, H α-quinoline), 5.35 (d, ^3J = 12 Hz, 1 H, CH_2 ligand), 5.05 (d, ^3J = 13 Hz, 1 H, CH_2 ligand), 4.86 (d, ^3J = 13 Hz, 1 H, CH_2 ligand), 4. 00 (d, ^3J = 12 Hz, 1 H, CH_2 ligand), 1.35 (s, 15 H, C_5Me_5); minor isomer: δ = 8.95 (d, ^3J = 5 Hz, 1 H, H α-quinoline), 5.53 (d, ^3J = 12 Hz, 1 H, CH_2 ligand), 5.01 (d, ^3J = 13 Hz, 1 H, CH_2 ligand), 4.89 (d, ^3J = 13 Hz, 1 H, CH_2 ligand), 4.17 (d, ^3J = 12 Hz, 1 H, CH_2 ligand), 1.40 (s, 15 H, C_5Me_5) ppm. $C_{41}H_{37}ClF_6N_2PRh$ (841.07): calcd. C 58.55, H 4.43, N 3.33; found

 © 2008 Wiley-VCH Verlag GmbH & Co. KGaA, Weinheim

Table 4. Crystal data and structure refinement for **9** and **10a**.

	9	**10a**
Empirical formula	$C_{38}H_{37}ClF_6N_2RhSb$	$C_{42}H_{38}Cl_4F_6N_2PRh$
Formula mass	895.81	960.42
Crystal system	monoclinic	orthorhombic
Space group	$P2_1$	$P2_12_12_1$
a [Å]	7.8524(3)	9.0917(7)
b [Å]	16.0187(6)	11.415(1)
c [Å]	16.5083(7)	39.422(4)
β [°]	103.325(4)	
Volume [Å^3]	2020.6(1)	4091.4(6)
Z	2	4
Absorption coefficient [mm^{-1}]	1.197	0.779
θ range for data collection	3.81–26.00	4–25
Reflections collected	5026	17206
Independent reflections	3808 [R(int) = 0.0247]	6417 [R(int) = 0.0576]
Absorption correction	multi-scan (SAINT)	multi-scan (SAINT)
Refinement method	full-matrix least squares on F^2	full-matrix least squares on F^2
Data/restraints/parameters	3808/19/447	6417/46/509
Final R indices [$I > 2\sigma(I)$]	R_1 = 0.0406, wR_2 = 0.0958	R_1 = 0.0578, wR_2 = 0.1301
R indices (all data)	R_1 = 0.0542, wR_2 = 0.1028	R_1 = 0.0883, wR_2 = 0.1432
Absolute structure parameter	0.03(4)	–0.02(6)
Largest difference peak/hole [e Å^{-3}]	0.589/–0.469	0.698/–0.433

C 55.13, H 4.48, N 2.95. Conductivity (5×10^{-4} M, CH_3OH): Λ = 81 Ω^{-1} cm^2 mol^{-1}.

Nucleophilic Substitution Reaction: Bu_4NI (26 mg, 0.07 mmol) was added to a solution of [Ru(η^6-*p*-cymene)(N-N*)Cl]PF_6 [N-N* = (S_a)-**1** or (S_a)-**2**; 0.020 mmol] in MeOH (10 mL), and the colour changed from yellow to red-orange. The mixture was allowed to stand at 328 K for about 3 h then left to cool to ambient temperature and concentrated under vacuum. The residue was precipitated from CH_2Cl_2/hexane to give [Ru(η^6-*p*-cymene)(N-N*)I]PF_6 as a red solid.

Kinetics: The reactions were monitored in $CHCl_3$ containing variable amounts of methanol by recording UV spectra at 328 K during the timescale of the nucleophilic substitution. The kinetic runs were performed by adding a known volume of a 1 M Bu_4NI solution to a 5×10^{-4} M solution, containing different ratios of $CHCl_3$ with respect to MeOH of the complex [Ru(η^6-*p*-cymene)(S_a-**1**)Cl]-PF_6. The kinetics were studied under pseudo-first-order conditions with a nucleophilic concentration of at least 20 times that of the complex. The rate constants were calculated as the means of three kinetic runs.

Crystal Structure Determination of 9 and 10a: The intensity data for **9** and **10a** were collected at room temp. with a Bruker APEX 8 diffractometer equipped with a graphite-monochromated Mo-K_α radiation source and an area detector. The data collection, cell refinement and reduction were carried out with the SMART and SAINT programs.[26] The two structures were solved by direct methods with the Sir 2004 program[27] and refined by weighted full-matrix least-squares procedures based on F^2 (SHELX-97).[28] All non-hydrogen atoms were refined with anisotropic thermal parameters. The hydrogen atoms were introduced into the geometrically calculated positions and refined using a riding model. Crystallographic and experimental details are summarised in Table 4. CCDC-650960 and -650961 (for complexes **9** and **10a**, respectively) contain the supplementary crystallographic data for this paper. These data can be obtained free of charge from The Cambridge Crystallographic Data Centre via www.ccdc.cam.ac.uk/data_request/cif.

DFT Calculations: All calculations were carried out using the Gaussian G03W program package.[29] The geometries of all species were fully optimised at the density functional (DFT) level using the PBE1PBE hybrid density functional (based on the Perdew, Burke and Ernzerhof[30] correlation and exchange functionals, as modified by Adamo and Barone[31]) and the B3LYP hybrid density functional, which uses Becke's exchange functional and includes the Slater exchange along with corrections involving the density gradient;[23] Perdew and Wang's gradient-corrected correlation functional[24,25] was also applied. The quasi-relativistic effective core potentials (ECP) LANL2DZ and SDD were used with both functionals. Several other theoretical works on Ru^{II} complexes[32–34] with B3LYP and B3PW91 functionals as well as the second-order Moller–Plesset perturbation method give good agreement with the reported experimental data. In our case the PBE1PBE hybrid density functional together with the SDD basis set can provide structural parameters in excellent agreement with the experimental X-ray data and with a large number of parent complexes reported in the CSD.[35]

Acknowledgments

This work was supported by the Ministero dell'Istruzione, dell'Università e della Ricerca, Rome (MIUR-Rome; PRIN no. 2005035123).

[1] a) R. Noyori, in *Asymmetric Catalysis in Organic Synthesis*, Wiley, New York, **1994**; b) I. Omae, in *Applications of Organometallic Compounds*, Wiley, Chichester, U.K., **1998**, chapter 20; c) B. M. Trost, L. van Vranken, *Chem. Rev.* **1996**, *96*, 395–422; d) H. Brunner, *Angew. Chem. Int. Ed.* **1999**, *38*, 1194–1208; e) I. Ojima, *Catalytic Asymmetric Synthesis* VCH Publishers, New York, **1993**; f) B. M. Trost, C. Lee, in *Catalytic Asymmetric Synthesis* (Ed.: I. Ojima), 2nd ed., Wiley-VCH, New York, **2000**, p. 593–649; g) *Comprehensive Asymmetric Catalysis*, vols. I–III (Eds.: E. N. Jacobsen, A. Pfaltz, H. Yamamoto), Springer-Verlag, Berlin, **1999**; h) L. Mimassi, C. Guyard-Duhayon, M. Noelle Rager, H. Amouri, *Inorg. Chem.* **2004**, *43*, 6644; i) L. Mimassi, C. Cordier, C. Guyard-Duhayon, B. E. Mann, H. Amouri, *Organometallics* **2007**, *26*, 860.

[2] For recent reviews, see: a) H. Brunner, *Eur. J. Inorg. Chem.* **2001**, 905–912; b) C. Ganter, *Chem. Soc. Rev.* **2003**, *32*, 130–138.

 © 2008 Wiley-VCH Verlag GmbH & Co. KGaA, Weinheim

[3] a) R. Noyori, H. Takaya, *Acc. Chem. Res.* **1990**, *23*, 345–350; b) V. Ritleng, M. Pfeffer, C. Sirlin, *Organometallics* **2003**, *22*, 347–354; c) F. Hapiot, F. Agbossou, A. Mortreux, *Tetrahedron: Asymmetry* **1994**, *5*, 515–518; d) K. Murata, H. Konishi, M. Ito, T. Ikariya, *Organometallics* **2002**, *21*, 253–255; e) K. Wan, M. E. Davis, *Tetrahedron: Asymmetry* **1993**, *4*, 2461–2468; f) M. R. Meneghetti, M. Grellier, M. Pfeffer, J. Dupont, J. Fischer, *Organometallics* **1999**, *18*, 5560–5570; g) J. W. Faller, K. J. Chase, *Organometallics* **1995**, *14*, 1592–1600; h) J. W. Faller, D. G. D'Alliessi, *Organometallics* **2003**, *22*, 2749–2757; i) P. Pinto, G. Marconi, F. W. Heinemann, U. Zenneck, *Organometallics* **2004**, *23*, 374–380; j) A. Davenport, D. L. Davies, J. Fawcett, D. R. Russell, *Dalton Trans.* **2004**, 1481–1492; k) H. Brunner, T. Zwack, M. Zabel, W. Beck, A. Bohm, *Organometallics* **2003**, *22*, 1741–1750; l) V. Alezra, G. Bernardinelli, C. Corminboeuf, U. Frey, E. P. Kündig, A. E. Merbach, C. M. Saudan, F. Viton, J. Weber, *J. Am. Chem. Soc.* **2004**, *126*, 4843–4853; m) Y. Kataoka, Y. Nakagawa, A. Shibahara, T. Yamagata, K. Mashima, K. Tani, *Organometallics* **2004**, *23*, 2095–2099; n) A. Doppiu, U. Englert, A. Salzer, *Chem. Commun.* **2004**, 2166–2167; o) H. Brunner, A. Köllnberger, A. Mehmood, T. Tsuno, M. Zabel, *Organometallics* **2004**, *23*, 4006–4008; p) E. Cayuela, F. Jalón, B. R. Manzano, G. Espino, W. Weissensteiner, K. Mereiter, *J. Am. Chem. Soc.* **2004**, *126*, 7049–7062; q) L. Qiu, F. Y. Kwong, J. Wu, W. H. Lam, S. Chan, W. Y. Yu, Y. M. Li, R. Guo, Z. Zhou, A. S. C. Chan, *J. Am. Chem. Soc.* **2006**, *128*, 5955–5965.

[4] C. G. Arena, S. Calamia, F. Faraone, C. Graiff, A. Tiripicchio, *J. Chem. Soc. Dalton Trans.* **2000**, 3149–3157.

[5] D. Drommi, F. Faraone, G. Franciò, D. Belletti, C. Graiff, A. Tiripicchio, *Organometallics* **2002**, *21*, 761–764.

[6] D. Drommi, M. Saporita, G. Bruno, F. Faraone, P. Scafato, C. Rosini, *Dalton Trans.* **2007**, 1509–1519.

[7] a) B. Milani, F. Amoroso, M. R. Axet, E. Zangrando, F.Faraone, D. Drommi, M. Saporita, *VIII Netherlands' Catalysis and Chemistry Conference*, Noordwijkerhout, The Netherlands, **2007**, P 90; b) B. Milani, F. Amoroso, M. R. Axet, E. Zangrando, F. Faraone, D. Drommi, M. Saporita, manuscript in preparation.

[8] a) R. K. Rath, G. A. N. Gowda, A. R. Chakravarty, *Proc. Indian Acad. Sci. (Chem. Sci.)* **2002**, *114*, 461–472 and references cited therein; b) V. Ritleng, P. Bertani, M. Pfeffer, C. Sirlin, J. Hirschinger, *Inorg. Chem.* **2001**, *40*, 5117–5122 and references cited therein.

[9] H. Brunner, R. Oeschey, B. Nuber, *Inorg. Chem.* **1995**, *34*, 3349–3351.

[10] D. Cremer, J. A. Pople, *J. Am. Chem. Soc.* **1975**, *97*, 1354–1358.

[11] Cambridge Crystallographic Data Centre, V. 5.26: F. Allen, C. M. Bird, R. S. Rowland, P. R. Raithby, *Acta Crystallogr. Sect. B* **1997**, *53*, 696–701.

[12] a) T. S. Billson, J. D. Crane, D. Foster, C. S. L. Russel, E. Sinn, S. J. Teat, N. A. Young, *Inorg. Chem. Commun.* **1999**, *2*, 476–478; b) S. Doherty, J. G. Knight, T. H. Scanlan, M. R. J. Elsegood, W. Clegg, *J. Organomet. Chem.* **2002**, *650*, 231–248; c) M. Shi, G.-X. Lei, Y. Masaki, *Tetrahedron: Asymmetry* **1999**, *10*, 2071–2074.

[13] a) D. S. Glueck, R. G. Bergman, *Organometallics* **1991**, *10*, 1479–1486; b) E. L. Muetterties, J. R. Bleeke, E. J. Wucherer, T. A. Albright, *Chem. Rev.* **1982**, *82*, 499–525; c) J. M. O'Connor, C. P. Casey, *Chem. Rev.* **1987**, *87*, 307–318.

[14] J. Wolf, H. Werner, D. Serhadli, M. L. Ziegler, *Angew. Chem. Int. Ed. Engl.* **1983**, *22*, 414–416.

[15] a) H. Brunner, *Adv. Organometallics Chem.* **1980**, *18*, 151–206; b) Y. Matsushima, K. Onitsuka, S. Takahashi, *Organometallics* **2005**, *24*, 2747–2754; c) H. Brunner, J. Aclasis, M. Langer, W. Steger, *Angew. Chem. Int. Ed. Engl.* **1974**, *13*, 810–811; d) H. Brunner, M. Langer, *J. Organomet. Chem.* **1975**, *87*, 223–240; e) H. Brunner, W. Steger, *J. Organometallics Chem.* **1976**, *120*, 239–256; f) H. Brunner, J. A. Aclasis, *J. Organomet. Chem.* **1976**, *104*, 347–362; g) G. C. Martin, J. M. Boncella, *Organometallics* **1991**, *10*, 2804–2811; h) H. E. Bryndza, J. P. Domaille, R. A. Paciello, J. E. Bercaw, *Organometallics* **1989**, *8*, 379–385; i) N. Gül, J. H. Nelson, *Organometallics* **1999**, *18*, 709–725; j) G. Consiglio, F. Morandini, *Chem. Rev.* **1987**, *87*, 761–778.

[16] S. Attar, V. J. Catalano, J. H. Nelson, *Organometallics* **1996**, *15*, 2932–2946.

[17] a) P. Hofmann, *Angew. Chem. Int. Ed. Engl.* **1977**, *16*, 536; b) P. Hamon, L. Toupet, J. R. Hamon, C. Lapinte, *Organometallics* **1996**, *15*, 10–12.

[18] M. A. Dewey, G. A. Stark, J. A. Gladysz, *Organometallics* **1996**, *15*, 4798–4807.

[19] a) M. Gomez, S. Jansat, G. Muller, G. Aullon, M. A. Maestro, *Eur. J. Inorg. Chem.* **2005**, 4341–4351; b) H. Brunner, F. Henning, M. Weber, M. Zabel, D. Carmona, F. J. Lahoz, *Synthesis* **2003**, 1091–1099.

[20] G. Brancatelli, M. Saporita, F. Nicolò, D. Drommi, F. Faraone, manuscript in preparation.

[21] T. Mecca, S. Superchi, E. Giorgio, C. Rosini, *Tetrahedron: Asymmetry* **2001**, *12*, 1225–1233.

[22] V. Sklenář, H. Miyashiro, G. Zon, H. T. Miles, A. Bax, *FEBS Lett.* **1986**, *208*, 94–98.

[23] A. D. Becke, *Phys. Rev. A* **1988**, *38*, 3098–3100.

[24] Burke, J. P. Perdew, Y. Wang, in *Electronic Density Functional Theory: Recent Progress and New Directions* (Eds.: J. F. Dobson, G. Vignale, M. P. Das), Plenum, New York, **1998** and references cited therein.

[25] J. P. Perdew, K. Burke, Y. Wang, *Phys. Rev. B* **1996**, *54*, 16533–16539.

[26] SMART, V. 5.060 and SAINT, V. 6.02 Software, Bruker AXS Inc., Madison, WI, **1999**.

[27] M. C. Burla, R. Caliandro, M. Camalli, B. Carrozzini, G. L. Cascarano, L. De Caro, C. Giacovazzo, G. Polidori, R. Spagna, *J. Appl. Cryst.* **2005**, *38*, 381–388.

[28] G. M. Sheldrick, *SHELX-97*, *Program for the Solution and Refinement of Crystal Structures*, University of Göttingen, Germany, **1997**.

[29] M. J. Frisch, G. W. Trucks, H. B. Schlegel, G. E. Scuseria, M. A. Robb, J. R. Cheeseman, J. A. Montgomery, Jr., T. Vreven, K. N. Kudin, J. C. Burant, J. M. Millam, S. S. Iyengar, J. Tomasi, V. Barone, B. Mennucci, M. Cossi, G. Scalmani, N. Rega, G. A. Petersson, H. Nakatsuji, M. Hada, M. Ehara, K. Toyota, R. Fukuda, J. Hasegawa, M. Ishida, T. Nakajima, Y. Honda, O. Kitao, H. Nakai, M. Klene, X. Li, J. E. Knox, H. P. Hratchian, J. B. Cross, V. Bakken, C. Adamo, J. Jaramillo, R. Gomperts, R. E. Stratmann, O. Yazyev, A. J. Austin, R. Cammi, C. Pomelli, J. W. Ochterski, P. Y. Ayala, K. Morokuma, G. A. Voth, P. Salvador, J. J. Dannenberg, V. G. Zakrzewski, S. Dapprich, A. D. Daniels, M. C. Strain, O. Farkas, D. K. Malick, A. D. Rabuck, K. Raghavachari, J. B. Foresman, J. V. Ortiz, Q. Cui, A. G. Baboul, S. Clifford, J. Cioslowski, B. B. Stefanov, G. Liu, A. Liashenko, P. Piskorz, I. Komaromi, R. L. Martin, D. J. Fox, T. Keith, M. A. Al-Laham, C. Y. Peng, A. Nanayakkara, M. Challacombe, P. M. W. Gill, B. Johnson, W. Chen, M. W. Wong, C. Gonzalez, J. A. Pople, *Gaussian 03*, revision C.02, Gaussian, Inc., Wallingford, CT, **2004**..

[30] J. P. Perdew, M. Ernzerhof, K. J. Burke, *Chem. Phys.* **1996**, *105*, 9982–9985.

[31] C. Adamo, V. J. Barone, *Chem. Phys.* **1999**, *110*, 6158–6170.

[32] D. A. Alonso, P. Brandt, S. J. M. Nordin, P. G. Andersson, *J. Am. Chem. Soc.* **1999**, *121*, 9580–9588.

[33] D. G. I. Petra, J. N. H. Reek, J.-W. Handgraaf, E. J. Meijer, P. Dierkes, P. C. J. Kamer, J. Brussee, H. E. Schoemaker, P. W. N. M. Van Leeuwen, *Chem. Eur. J.* **2000**, *6*, 2818–2829.

[34] M. Yamakawa, H. Ito, R. Noyori, *J. Am. Chem. Soc.* **2000**, *122*, 1466–1478.

[35] F. H. Allen, *Acta Crystallogr. Sect. B* **2002**, *58*, 380–388.

Received: July 9, 2007
Published Online: October 31, 2007

 © 2008 Wiley-VCH Verlag GmbH & Co. KGaA, Weinheim